Assessment of the Urban Heat Island in Biel/Bienne

Master thesis
Faculty of Science, University of Bern

handed in by

Gabrial Thor Makai Erismann

2025

Supervisor

Prof. Dr. Stefan Brönnimann
and
Dr. Moritz Gubler

Contents

Chapter 1

Introduction

Global warming and urbanization are two key features of the 20th and 21st centuries. The Urban Heat Island (UHI), the difference between temperatures in an urbanized area and the surrounding countryside, has therefore suscitated interest by the public, governments and researchers around the world. Through setting up an in-situ sensor network to measure air temperature from May - September 2023, this present work provides an overview of the UHI and related heat indicators in the main urban areas of the Biel agglomeration. The results of urban climate research in Biel in the 1980s are used to provide context and to guide investigation into sources of cold air to relieve high night-time temperatures in the city. In addition the results from an urban heat model released in 2023 for all urbanized areas in the canton of Bern are compared to the empirical network to evaluate the model's efficacy in the complex topography of the city of Biel. Hopefully this research will be of use to urban planners in the city of Biel, and all *Biennois.e* and *Bierer.in* interested in their urban climate, but also serve as another one of many comparison points for researchers working on UHI across Europe and globally.

The highest authority on climate change research, the Intergovernmental Panel on Climate Change (IPCC), states unequivocally that global warming is already having severe effects on human society in the present day and that this warming trend will continue to drive increased climate-related risks in the future (IPCC, 2023). According to data from the UC Berkeley climate research group, 2023 was the first year where global temperatures surpassed 1.5°C above the pre-industrial baseline (Berkeley Earth, 2024). In Switzerland, authorities report a 2°C increase in near-surface air temperature from the pre-industrial baseline to 2017 (compared to 0.9°C overall), and both predict further warming and expect more intense heatwaves (MeteoSwiss, 2018 and Casanueva et al., 2023). While climate change will not affect the magnitude of urban-rural temperature differences, it increases the baseline temperature in rural areas. This make further temperature increases due to the UHI effect more dangerous in terms of impact on human health and well-being, underlining the importance of understanding the UHI's distribution and magnitude.

By definition the UHI impacts urban populations. Today, the majority of the global population lives in cities and this is projected to grow to 70-80 percent in the coming decades (Elmqvist et al., 2013). In Switzerland, as in much of the developed world, around 80 percent of the population is already urban: there are 5.6 million people in an *urban core*, 1.9 million people in *areas affected by an urban core*, and 1.3 million people *beyond urban core influence* (Swiss Federal Statistical Office (BFS), 2024b). In the canton of Bern, of which Biel is the second largest city, these figures are 0.6 million, 0.2 million and 0.2 million respectively, or about 80 percent of the population living in an urbanized area, broadly similar to the country as a whole (Swiss Federal Statistical Office (BFS), 2024b). As such, most Swiss inhabitants are affected by the issue of the urban heat island to a greater or lesser extent. While the drivers of urban climate are well understood thanks to decades of research, a particular urban climate is unique to its location, climate, topography, city size, physical structure,

building materials and more (Oke et al., 2017). This underscores the importance of providing local empirical data to support urban planning and decision-making across the heterogenous Swiss urban landscape.

The main threat posed by the urban heat island is the potential for negatively impacting human health and well-being. Europe's first and worst heatwave of the 21st century caused up to 70,000 moralities across the continent and exemplified the risks facing Europe in a future dominated by climate change (Robine et al., 2008). In 2005, Swiss researchers estimated that all-cause mortality increased as much as 7 percent during the June to August heatwave period and correlated the deaths spatio-temporally with recorded high temperatures, suggesting the proximate cause of death was indeed increased temperatures (Grize et al., 2005). Even in the absence of such extremes, research suggests relatively minor heat events and prolonged exposure to increased ambient temperatures causes upticks in summertime all-cause mortality of between 3 and 5 percent in Switzerland (M. S. Ragettli et al., 2017 and Vicedo-Cabrera et al., 2023 and M. Ragettli et al., 2020). The UHI has been found to lead to increased mortality in European cities, with effects on mortality in the same range as those of common air pollutants (ozone and PM_{25}) (Huang et al., 2023). As Switzerland's population continues to age, the proportion at increased risk of heat related morbidity rises as well (de Schrijver et al., 2022). From a health and well-being perspective, it is clear that understanding the UHI grows in importance as temperatures rise, urbanization continues, and populations age.

Swiss federal and local authorities have developed strategies and issued guidance to mitigate the UHI across Switzerland, often through research collaborations with local universities (Bundesamt für Umwelt (BAFU), 2018 and Ville de Genève, 2024 and Stadt Bern, 2024 and Stadt Zürich, 2024). In some cities, such as Bern where the University of Bern's Urban Climate research group, partnered with municipal authorities, there is significant research, empirical data collection, and even competing models of the UHI available for the public and for planners.[1] In other cities, there is much less data available, and much of the data comes from modeling, in particular the FITNAH (Flow over Irregular Terrain with Natural and Anthropogenic Heat Sources) 3D Model developed by the German company Geonet. The cantons of Bern, Luzern, Neuchâtel, Aarau, Solothurn, Geneva and others used have all contracted a UHI model within the past two years to provide all of their communes, including Biel, with gridded urban heat island data (Geonet, 2023b and Geonet, 2024a and Geonet, 2024b and Geonet, 2022, Geonet, 2023a and Système d'Information du Territoire à Genève (SITG), 2024). While the wide availability of this modeled data is laudable, UHI models have significant limitations and benefit from the feedback of an empirical reference network for both parametrization and verification, as demonstrated by model comparison work done in Bern, which included the results of the FITNAH model (Burger, Gubler, et al., 2024). The 2023 empirical network in Biel provides therefore a useful comparison point for a UHI reference that is used by local planners across Switzerland.

In sum, this research on the UHI in Biel is highly relevant. Understanding the spatial and temporal distribution of the UHI, affecting some four out of five Swiss permanent residents, only grows in importance as the Swiss population ages and global warming raises baseline temperatures. While Switzerland's larger cities (notably Bern, Zurich and Basel) have reliable empirical data, this is not the case in Switzerland's smaller cities, such as Biel; this gap is now being filled with data from the FITNAH model. A new series of summer-long data from a dense, in-situ network is therefore relevant for planners in Biel and for other cities in Switzerland looking to leverage the availability of the FITNAH dataset

[1] Much of this work is available on the GIUB *Stadtklima* website through theses that may or may not be available to the public. The interested reader can request access to these works.

1.1 The Urban Energy Balance

The UHI is the most studied facet of *urban climate*, which describes any climatic property that differs systematically in an urban area compared to the surrounding countryside (Kuttler, 2008). In atmospheric science, the term urban boundary layer (UBL) refers to the section of the atmosphere that has been directly affected by changing the land use from rural to urban, for example by constructing streets and buildings (Oke et al., 2017). In the vertical direction, this stretches from the ground up to one or two kilometers during the day and on the order of dozens to hundreds of meters at night under ideal conditions (Oke et al., 2017). Like other indicators of urban climate, the UHI effect is strongest near the urban surface. The empirical network in this study uses sensors placed at a height of three meters and the model data used in this study is of air temperature at a height of two meters, both of which lie towards the bottom of the Urban Canopy Layer (UCL), as shown in Figure 1.1.

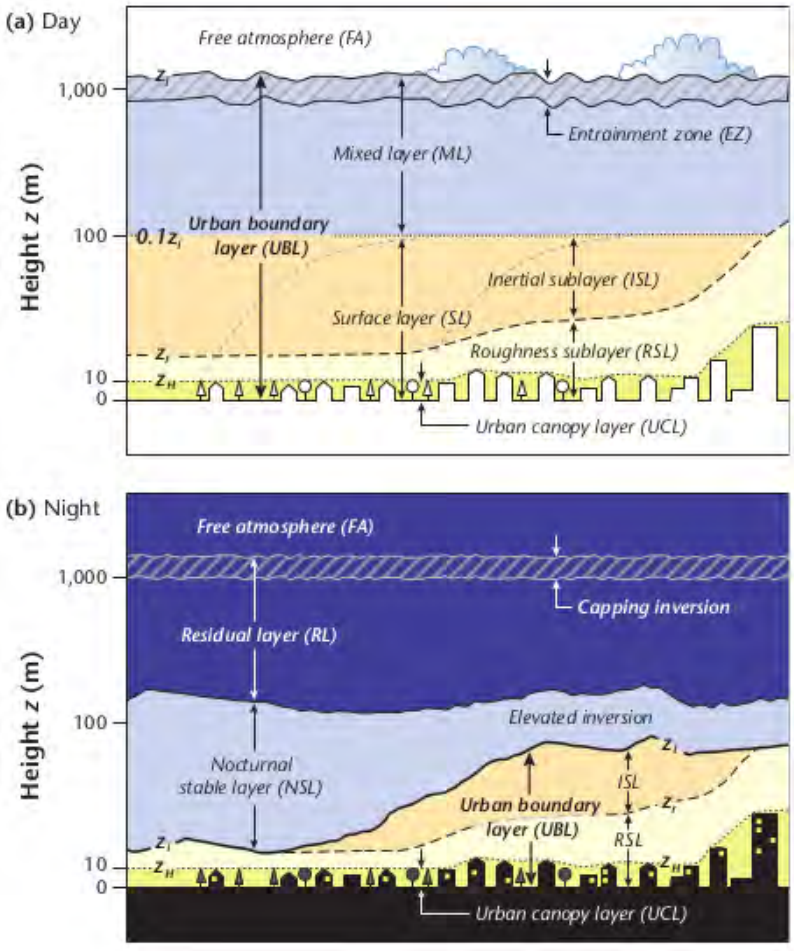

Figure 1.1: Schematic of different atmospheric layers in the city under ideal day and night meteorological conditions. The empirical data in this study comes from sensors 3m high and the model data used is calculated for a two meter height so the entire study takes place at the bottom of the Urban Canopy Layer. Source: (Oke et al., 2017) page 31

A typical UHI reaches a maximum in the early morning, during the coolest part of the day,

and has a minimum around solar noon, during the warmest part of the day (Oke, 1982). One interpretation of the UHI therefore, is as a slower rate of cooling of urban areas compared to the surrounding countryside. During the day, both the city and its surroundings receive similar amounts of energy in the form of solar radiation and therefore reach similar maximum temperatures, but the city is less able to release this energy back into the atmosphere at night resulting in elevated early morning temperatures. As put in Oke, 1982 when comparing the UHI of large, global cities "Ceteris paribus the relevant and therefore critical properties governing these differences [the timing of heat-release] are the radiation geometry [...] and the surface thermal properties [...]. The radiation geometry refers to the height, location and density of buildings that both increases the surface area for absorption of short-wave radiation and blocks the release of energy over the night by long-wave radiation (Oke, 1981). Radiation can escape directly into the sky unobstructed by buildings in rural areas, while in cities the building geometry absorbs and reflects back this radiation thus slowing the cooling process (Oke, 1981). The surface thermal properties refer to the increased capacity of common building materials to both absorb and retain more of the solar energy received during the day compared to a vegetative land cover found in rural areas (Oke, 1982).

However, there are many other factors that affect the magnitude of the UHI over the course of the day. Air pollution can both reduce the amount of incoming direct solar radiation that reaches the urban surface and decrease the ability of long-wave radiation to escape the UCL (Oke et al., 2017). The former could potentially lower the UHI and the latter could increase it. Another driver of the UHI is the effect of heat directly produced by human activity, for example air conditioner exhaust, industrial activities, vehicle traffic, or indoor heating (Brönnimann, 2018). The effect of this can vary widely from having signficant local effects to being barely detectable. A third factor is the availability of moisture. The latent energy transfer, or energy consumed when water evaporates, is reduced by urbanization since one of the defining features of urbanization is the conversion of permeable ground with vegetation into impermeable built materials that prevent evapotranspiration (Brönnimann, 2018). Another large factor is the obstruction of airflow that can reduce the ability of horizontal and vertical advection of hot air, leading to a concentration of hot air in hotspots through a city (Oke et al., 2017). The influence of each of these factors can vary greatly from important to negligible depending on the season, the time of day, and the structure of the city itself.

The UHI is also a function of the weather on that day. Stormy days have a much reduced UHI compared to clear, sunny days, even during the peak early morning hours. Clouds reflect long-wave radiation back to the ground in rural and urban areas alike, thereby lowering the cooling rate of rural areas, while strong winds can effectively evacuate warm air (Oke et al., 2017). In the opposite case, long term low-pressure systems that result in consistent high temperatures and low winds enhance the UHI due to the lack of moisture for latent heat transfer and reduced horizontal and vertical advection of hot air from urban areas (Oke et al., 2017). The weather therefore plays an inverted role to the one that might be desired - the UHI is augmented by heatwave conditions and reduced by stormy summer weather.

Local geography plays a role as well. Being adjacent to a high mountain range will affect precipitation and wind patterns and coastal cities benefit from onshore-offshore winds that can regulate the urban climate (Oke et al., 2017). Smaller scale topographical features can also affect the urban climate by physically blocking circulation patterns that may accentuate features of the urban climate. Cities located in valleys and depressions can often be at risk of high UHI and air pollution due to air becoming blocked by these features, while cities on the slope or crest of topographic features can see the opposite effect (Oke et al., 2017). Differential warming and cooling cause by different elevations also cause warm air to flow up slop during the day (anabatic winds) and cold air to flow downslope at night (katabatic winds), the latter of which can reduce the UHI, when its magnitude is highest. All together, a city's building geometry, material composition, distribution of human activities, local weather patterns, and topographic features influence the magnitude and distribution of the UHI.

1.2 Measuring the UHI

The most common and mpractical way to study the UHI is as the difference between some measure of air temperature over a desired timescale at an urban site T_u and surrounding rural sites T_r : $UHI = T_u - T_r$. (**UHIIntensity**). The fundamental assumption behind this approach is that the rural sensor(s) is (are) a good proxy for what the temperatures would be in the urban locations if the city had not been built. There are numerous ways to measure the UHI: via an in-situ sensor network, measurement transects across the city, remote sensing techniques, measurements of vertical air temperature via soundings, modeling and more (Oke et al., 2017). As the level of interest in urban climate and the UHI has grown, so has the level of detail in UHI studies as researchers attempt to capture more of the UHI variation within urban boundaries (**uhi˙variance**). In 2023, the World Meteorological Organization (WMO) issued guidelines on UHI measurements, which nonetheless leave significant leeway to the researcher in determining acceptable station siting characteristics depending on the purpose of the study; each researcher must decide how best to capture this phenomenon for their particular research question and intended audience (Organization, 2023 and **uhi˙variance**). Since the method chosen to measure the UHI in Biel was an in-situ network distributed throughout the city, the following discussion will focus on challenges to measuring accurately the UHI using such a network.

One advantage of a sensor network is that stations have continuous measurements in time throughout the study period, allowing it to effectively capture the diurnal and seasonal variation of the UHI. In the vertical dimension, there is no variation in a typical in-situ network, therefore there is no information on the vertical distribution of air temperatures. Horizontally, the sensor network is necessarily limited in spacial coverage horizontally due to practical constraints of funding and availability of suitable locations. Each sensor in the network therefore represents not only itself, but a block or even a neighborhood (Oke et al., 2017). On a micro scale, building an empirical network requires special consideration of the rural and urban stations as local biases abound (Oke et al., 2017). On a macro scale, one must consider regions of similar structures, known as the Local Climate Zones (LCZ), to ensure that the heterogeneity on the neighborhood scale is reflected in calculation of the UHI (Oke et al., 2017).

The selection of rural reference sites is critical because they are the baselines against which all other locations will be compared. A site must be "[sic] situated outside the constructed urban space or any surface that has been modified by asphalt, cement, etc., in order for anthropogenic heat to be negligible in its energy balance, for the sensible and latent heat to be as similar as possible to that of natural cover, and for the radiation balance to present albedos and emissivity coefficients that are also similar to those of a natural environment." (Martin-Vide et al., 2015). Finding a suitable reference site within a close area of the city can be challenging due to the presence of peri-urban areas, built infrastructure, and potential contamination of the site by warm air that originates in the city (Martin-Vide et al., 2015 and Organization, 2023). Evan agricultural sites are affected by seasonal changes due to agricultural activities (Organization, 2023). If the site is not close enough, part of the urban-rural difference attributed to the UHI may in fact be due to differential microclimatic features. In principle therefore, a rural station is essentially a WMO-standard meteorological station, reducing the subjective choice involved in choosing station location.

This is not the case for urban stations, where the objective is to measure the impact of the built environment on the air temperature. The urban climate is highly heterogeneous and dependent on the physical structure, material composition, and function of the immediate area (Oke et al., 2017 and Organization, 2023). Local Climate Zones (LCZs), see Figure 1.4, are widely used in the literature, and recomended by the WMO, to group these heterogenous features by height, density, surface materials and ground cover type into larger units of study(Stewart and Oke, 2012 and Organization, 2023). Researchers use the LCZs to guide sensor placement, with the objective being to locate sensors within one LCZ so it is not influenced by neighboring LCZs . On a microscale, the sensor should be in a location that is representative of the LCZ itself, so that local anomolies do not overdetermine

the temperature readings. In general, this means placing sensors as far away as possible (while still being representative of the neighborhood) from buildings and trees. In 2017, researchers released a tool to calculate the LCZs of any city using templates available through Google Earth Engine (Demuzere et al., 2021). The LCZ framework is not a perfect solution to the heterogeneity of cities as it is biased towards large, American cities (Wellinger et al., 2024). Nonetheless it is a useful tool to allow intercomparison of urban areas and understand UHI dynamics even if the LCZ framework is not used as a final deciding tool in sensor location.

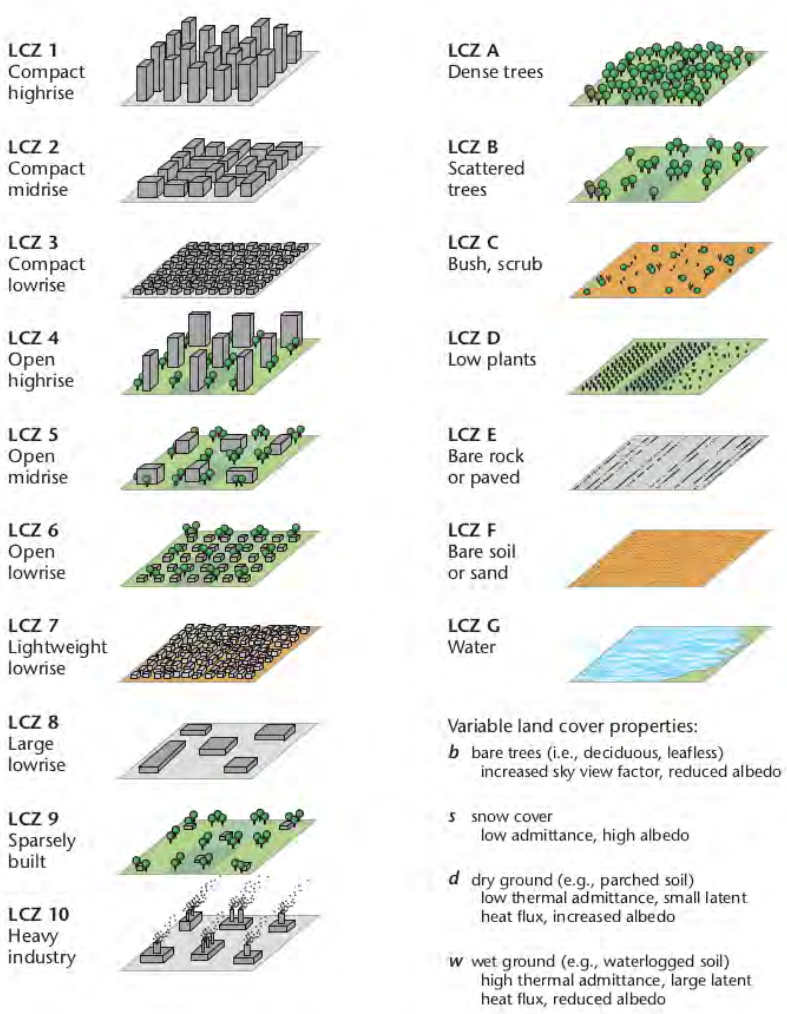

Figure 1.2: Standard Local Climate Zone (LCZ) classification as published in *Urban Climates* on page 26. In the Biel agglomeration, the LCZs 2, 5, 6, 8, 10, A, B, D, and G are identifiable.

Chapter 2

Location

Le climat doux et sain de Bienne, où la majorité des habitans arrive à un âge très-avancé, en fait un séjour fort convenable pour des cures de petit lait.

- *Guide du voyageur à Bienne et aux environs*, page 9.

2.1 Physical Geography and climate

The focus of this study is on the core of the urban zone comprising the city of Biel and the closest areas of the neighboring towns Port and Nidau, an area of around 25 square kilometers and 60'000 people (Swiss Federal Statistical Office (BFS), 2024a). Biel is located approximately 47.1368° N, 7.2468° E, and 430 meters above sea level. Biel lies at the border between the Swiss plateau and the Jura mountains, which descends slowly from the Swiss Alps about 100 kilometers to the South. Biel has a Köppen-Geiger climate classification of Cfb, that is a "warm temperate, fully humid, warm summer" (Kottek et al., 2006).

Biel is at the Northeastern end of a region known as the *seeland* which surrounds the three lakes of Neuchâtel, Murten and Biel and is the heart of Switzerland's agricultural production with relatively flat and fertile land. Lake Biel, which borders the city to the West, has seen sharply increasing water temperatures surpassing 25°C at the surface and 20°C at 20 meters depth during the warmest part of the annual cycle (Laboratoire cantonal de la protection des eaux et du sol, 2023). The lake drains through the city via the Thielle and Nidau-Bueren canals (200-300 meter / second combined streamflow), which have similar temperatures as the lake (Bundesamt für Umwelt BAFU, 2024a). The much smaller, colder and fast-moving Suze river enters Biel via the Taubenlochschlucht, runs through the center of the city, splits into three canals and drains into Lake Biel. However, the mean stream flow of the Suze was less than half of its typical monthly mean throughout the study period, which may decrease any potential cooling effect (Bundesamt für Umwelt BAFU, 2024b). Research on the impact of water bodies in and around urban areas suggests a mixed effect dependent on local conditions: often daytime uhi can go down as the water absorbs much of the heat, while nighttime UHI may be augmented by large bodies of water due to the release of stored daytime heat through convection and long-wave radiation (Steeneveld et al., 2014).

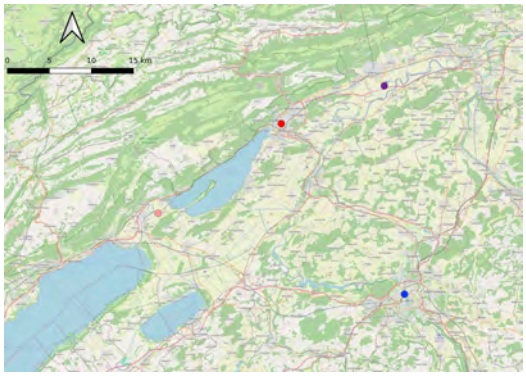

(a) Biel and neighboring weather stations

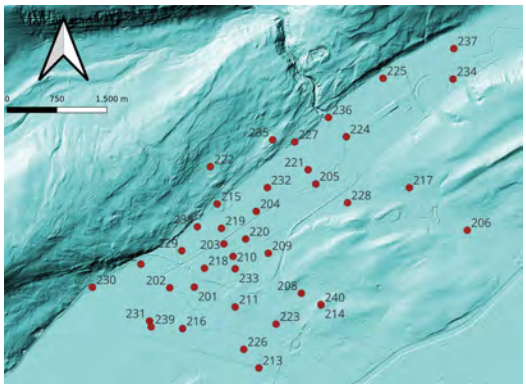

(b) Hillshade plot of Biel

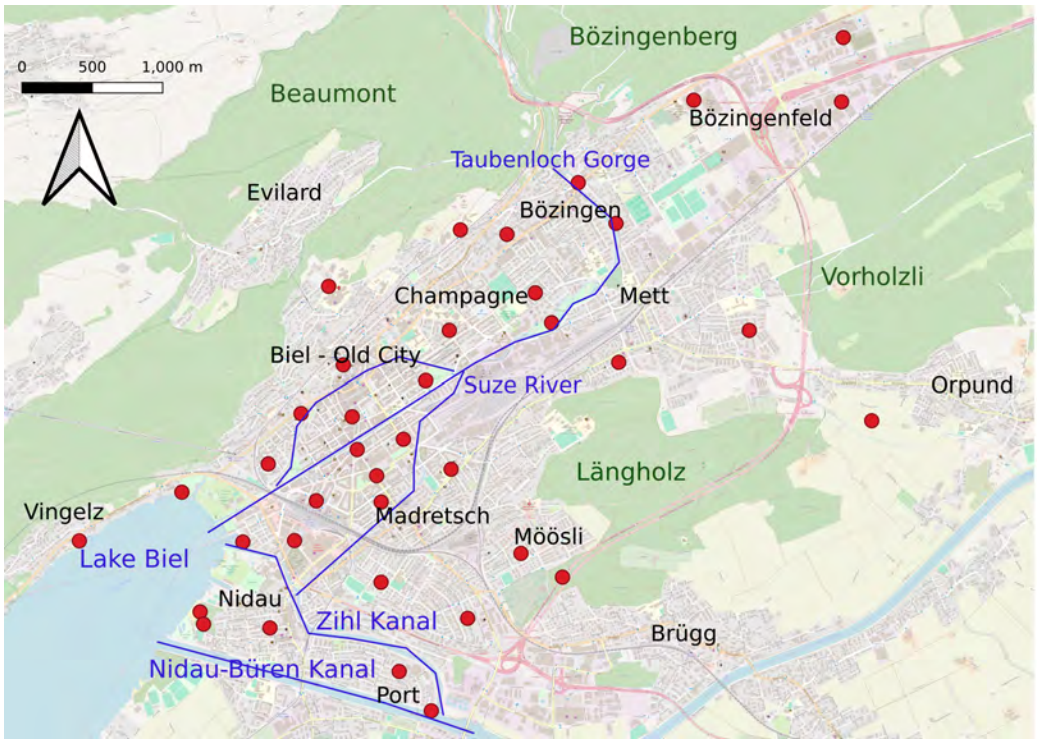

(c) Detailed map of Biel and surroundings

Figure 2.1: (a) The city of Biel is marked in Red, the Cressier NE weather station is marked in pink, the Grenchen GE station is marked in purple, and the Bern/Zollikofen BE station is marked inBlue. Also visible are the three lakes of Neuchatel, Biel, and Morat, making up the *Seeland* region. (b) A hillshade plot showing Biel's key topographical characteristics. The flatness of the city contrasts with wooded hills (the Längholz and Vorholzli) to the south and the Jura mountains to the north. Generated using two-meter resolution digital elevation model data from SwissTopo and QGIS 3.38.3-Grenoble. (c) A close-up map of Biel and its surroundings, indicating neighborhoods and communes (black), forested areas (green), and water features (blue). Urbanized areas extend beyond the sensor network to the southwest. Baseline data from Open Street Map API.

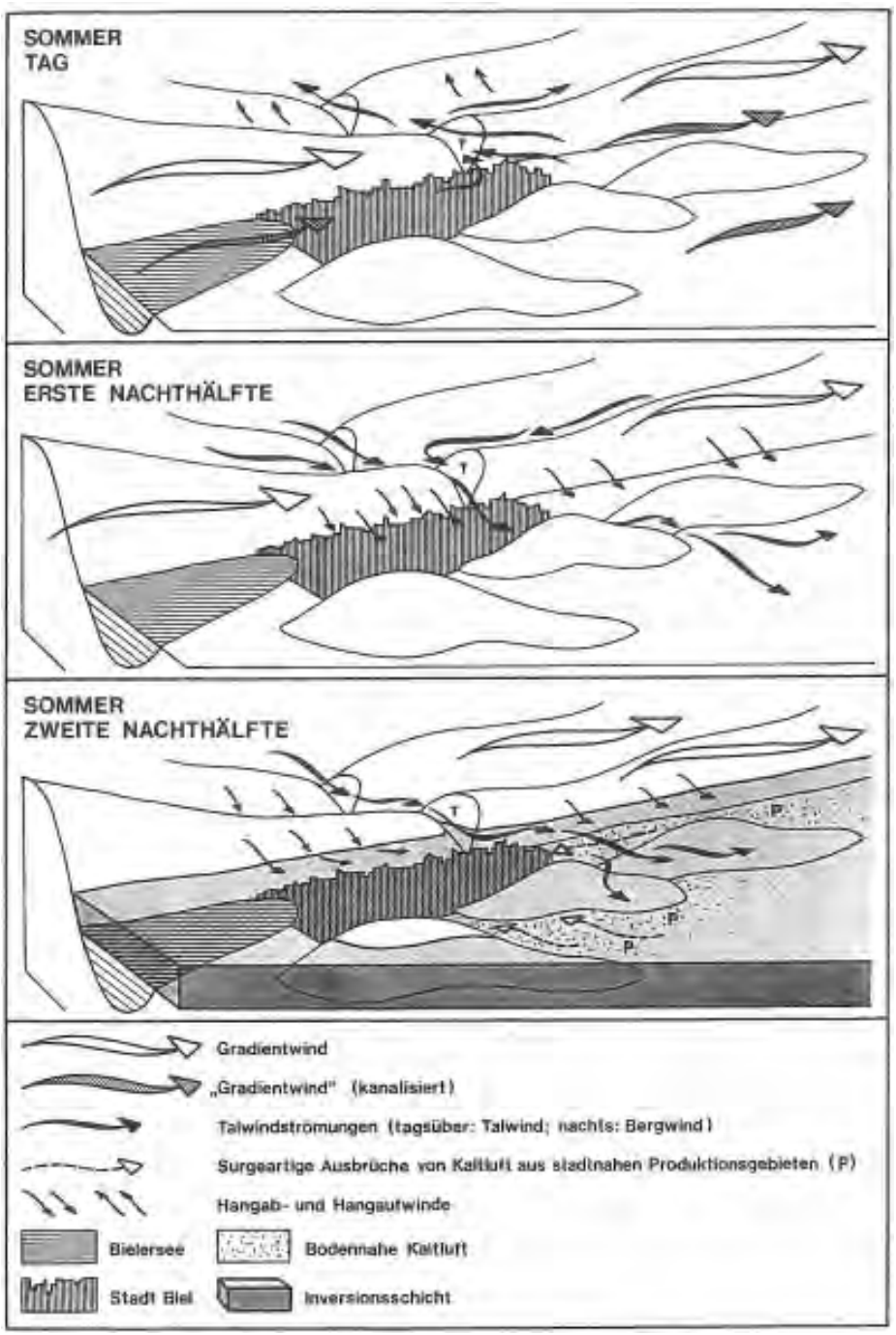

Figure 2.2: This image from Wanner, 1991, show the daily evolution of the UHI in the city of Biel and the direction of wind flow across the city. The top image is the summer day, the second image is the first half of a summer night, and the third image of the second half of a summer night. The prevailing wind in the West-East axis, channeled by the plateau and the Jura, is represented by the large white arrows. The flow of the wind from the Jura mountains is represented by the thick black arrows, and the flow of katabatic winds is represented by the small black arrows. The dashed arrows on the dotted land represents the flow cold air production into the city during the second half of the night.

The city is dominated by the Jura mountain range, which abuts Biel to the North and extends hundreds of kilometers to the North, Northwest and Northeast. A local culminating point of the Jura, the Chasseral, is located 15 kilometers to the Northwest, which is connected to the city via the valley of St. Imier, ultimately draining both cold air and the Suze river through the narrow Taubenloch gorge located at the Eastern end of the city in the Bözingen neighborhood. The city is built partially up the slopes of the first two mountains of the range, Beaumont (summit of 730 meters) and Bözingenberg (summit of 930 meters). The majority of the city however, is built on the old floodplain of the Suze river, thus the greatest part of the city is almost perfectly flat extending from Lake Biel in the West to Bözingenfeld in the East. The South and Southeast borders of the city are defined by the Längholz and the Vorholzli, two partially settled forested hills. See Figure 2.1 for a full With maximum elevations of about 490 and 540 meters respectively, this topographical configuration could cause Biel to experience a build up of warm air and pollution in the main parts of the city due to the physical obstructions in nearly all directions.

Local topography's impact on airflow in and around Biel was extensively studied in the 1980s exactly due to high levels of air pollution observed in the city (Wanner, 1991). On a macroscale, the orientation of the Jura mountain range and that of the Swiss Plateau leads to a Southwest / Northeast wind, which is often strongest in the Western part of Biel due to the smooth surface of the lake (Rickli, 1988). Potential sources of cold air flow have local obstructions that were found to hinder the passage of cold air through the city, especially during the second part of the night (Rickli, 1988). The idealized impact of these local features on air flow during a sunny summer day is presented in Figure 2.2 (Wanner, 1991). Katabatic winds caused by cold air descending down the Beaumont and Bözingenberg peak in the first half of the night and slow down by the early morning (Rickli, 1988). The valley of Saint Imier in the Jura North of Biel/Bienne channels cold air originating in the Jura along the Suze river valley, through the Taubenloch Gorge leading to an infiltration of cold air along the Suze river channel. Unfortuantely, this air can be deflected South East in the Orpund direction (Rickli, 1988). To the South, surface winds approach the city in the morning from the Plateau, but can be obstructed by the Vorholzli and the Längholz (Rickli, 1988).

2.2 Urban Development

The Eastern end of Lake Biel has been inhabited since the neolithic (Dubler & Martin, 2018). First mentioned in the written record in 1142, Biel was granted the status of city by the Bishop of Basel in 1230 (Dubler & Martin, 2018). By 1900, the population of Biel grew to 30'000 inhabitants, largely due to the influx of workers from the Jura bernois to work in the burgeoning industrial sector Berlincourt, 1988. Biel soon merged with the neighboring communes of Mett/Mâche, Bözingen/Boujean, Vigneules/Vingelz and Madretsch to form the modern boundaries of the city with a total 21 square kilometers (Berlincourt, 1988). Prior to World War I, local planners favored dense development of these cores along with industrial expansion along the Suze river (Berlincourt, 1988). During the interwar period areas between the city centers were filled in, followed by suburbanization composed of units for 1-3 families as well as the construction of small groups of large modernist residential complexes in the post-war period (Berlincourt, 1988). Up until the late 1960s Biel was a fast growing city and a manufacturing hub, dominated by the watch industry and attracting labour from across Switzerland and Italy. The city faced an acute and ongoing industrial crisis from the 1970s through the 1990s, when much of the industry, especially watch making and related subsidiary firms, that characterized Biel over the 20th century disappeared (Morisson & Gong, 2024). Population declined from a peak in 1968 of 64'000 to a low of 48'000 in 2001 (Dubler & Martin, 2018).

Over the past 20 years however, Biel has managed to successfully reinvigorate itself in the new services industry, consolidated the watch industry and is making plays in 'industry 4.0' (Morisson & Gong, 2024). Emblematic of this change is the transformation of the area behind the train station from an industrial zone dominated by a General Motors automotive factory (still in operation at the

time of the previous urban climate studies in Biel)into a shopping center with ongoing construction of a institution of higher education currently underway (located at sensor 201). The city's population grew back to 55'000 in 2020, with the urban agglomeration reaching 108'777 (Swiss Federal Statistical Office (BFS), 2024a). As part of this growth Biel has engaged in a number of urban greening and redevelopment projects that have changed the landscape in certain areas significantly since the 1980s (Hadorn, 2012). The most notable of these is the naturalization of the Ile de la Suze park (sensor 205) which created a large, pleasant green space along the Suze river in the heart of the city, for which the city won numerous prizes ("Schüssinsel", n.d.). The development of the Congress Center / Esplanade (sensor 210) from a large, central parking lot into a shopping and living center with wide green spaces, newly planted trees and white gravel is an example of the modern urban space with which the city is looking to present itself (Hadorn, 2012). The same can be said for the neighboring Madretschkanal developments (sensor 220) which also favored multi-story buildings with wide green spaces and gravel areas "Ein neues Stück Stadt", n.d.). There was also a push to include ecological measures in the development of the Bözingen industrial zone (Sensors 225, 237 and 234), in particular the widespread use the plantation of native meadows. [1]

As Biel has recovered economically and formerly disused areas are claimed for development, community activits have worked both with the city and in opposition to the city to build their own vision of a modern Biel. One example of cooperation where urban climate was cited as a deciding factor, is the Parc-de-la-Passerelle, a small community garden and lawn that was agreed to be preserved by the Madretsch guild and by the city of Biel [2]. Past cooperation has since turned into tension at the Terrain Gurzelen, formerly a sports stadium and now a large community garden and general use space for the local community, where organizers are attempting to blocks its development into housing units ("Terrain Gurzelen Home", n.d.). The Ile de la Suze passed overwhelmingly by popular vote, while a recent attempt to renovate the lower part of the river and turn it into a more accessible green area was rejected by voters this year. In January 2023 the Urban Climate Initiative, which envisions progressively transforming 10 percent of the existing road network into pedestrian, bike, bus or green infrastructure over ten years, was successfully deposed in front of largely supportive Biel authorities which should begin investments in this direction in 2025 (RJB, 2023). Other efforts have seen strong(er) political divisions, such as the successful campaign to stop the A5 highway which was destined to cut through the city, thus converting buildings and green space into highway infrastructure (West Ast, 2024).

The urban climate research in the 1980s provides an invaluable snapshot of the UHI when Biel was still predominantly an industrial town forty years ago. While the focus was on air pollution and not the UHI, and much of it took place during the winter months, research on the heat distribution during the summer months was also carried out Wanner, 1991. Researchers studied horizontal temperature fields using transects, vertical temperature fields and fixed measurement stations Rickli and Wanner, 2019. The maximum UHI effect was estimated to be between 6 - 7 ˚ C located in the densest part of the city near the old town(Rickli, 1988 and Wanner, 1991) The contour plots generated from transect data reproduced in Figure 2.3 show a signficant island of warmth in the area between the Suze river and the lake in the early hours of the morning and in the early evening (Wanner, 1991). The highest temperature differences are focused in the densest part of the urban core with the effect especially pronounced in the evening (bottom right figure of Figure 2.3).

[1] This information comes from correspondence with someone active in the debates surrounding the zoning and approval during the 1990s.

[2] I am a member of the association which maintains this garden and this is based on my personal observations.

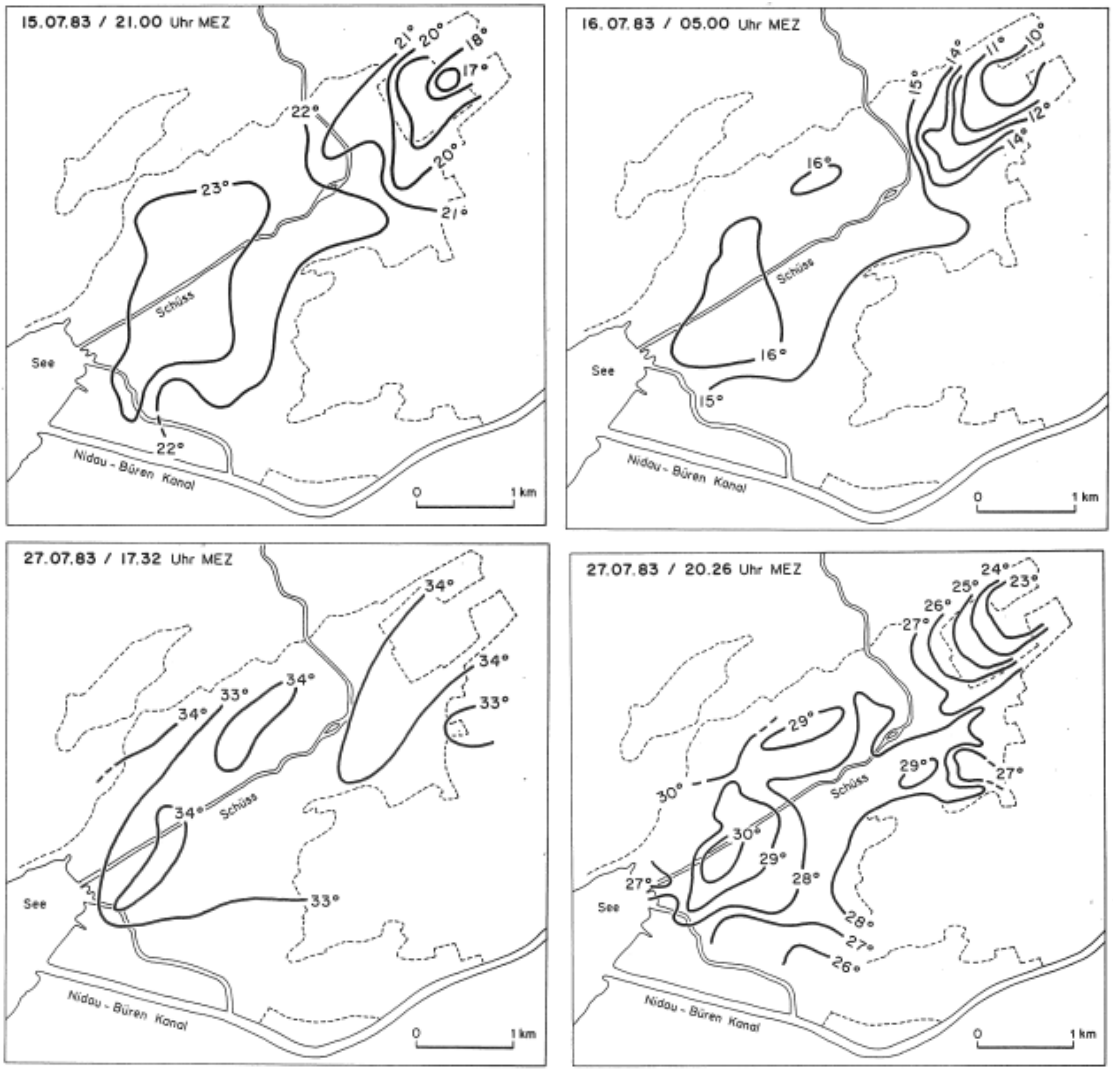

Figure 2.3: Horizontal temperature fields from the Urban Climate studies of Biel in the 1980s as inferred from cross sectional measurement campaigns conducted at different times and on different dates in July 1983. Top left: Temperature field at 21:00 on July 15 1983; Top Right: Temperature field at 05:40 on July 16 1983; Bottom left: Temperature field at 17:32 on July 27 1983; Bottom right: temperature field at 20:26 on July 27 1983

Today, after all of these changes, the former city-centers of Madretsch, Mett and Bözingen are much less distinct from the rest of the city than its history of 20th century development would imply. Biel's industrial roots, by contrast, are still visible in the number of light and heavy industrial zones in and around the city. This can be clearly seen in an LCZ map of the city depicted in Figure 2.4. LCZ map was generated using the online LCZ generation tool (Stewart & Oke, 2012). The LCZs of Biel are mainly suburban 1-3 story constructions (LCZ 6), 3-7 story constructions (LCZ 5) in denser neighborhoods, 3-10 story dense buildings (LCZ 2) in the very heart of the city, and light and heavy industrial areas (LCZ8 and LCZ10 respectively). There are many instances of clusters of high rise buildings in otherwise low or medium-low rise areas leading to difficulties in classification. Similarly, the old cities of Nidau, Mett and Bözingen consist of only a few buildings making it difficult to distinguish them from the surrounding slightly lower density areas. The overall picture painted by

the LCZ map is a core of LCZ 5 and LCZ 2 corresponding to Madretsch, the Old City, and the area in between, surrounded by suburbs and industry (LCZ 6 and LCZ 8 / 10 respectively). It shows a heavy proportion of heavy and light industry located to the south, center and west of the city. Finally, it shows how far to the Southwest the urbanized area extends - about 2 kilometers beyond the last stations in this direction (216 and 213).

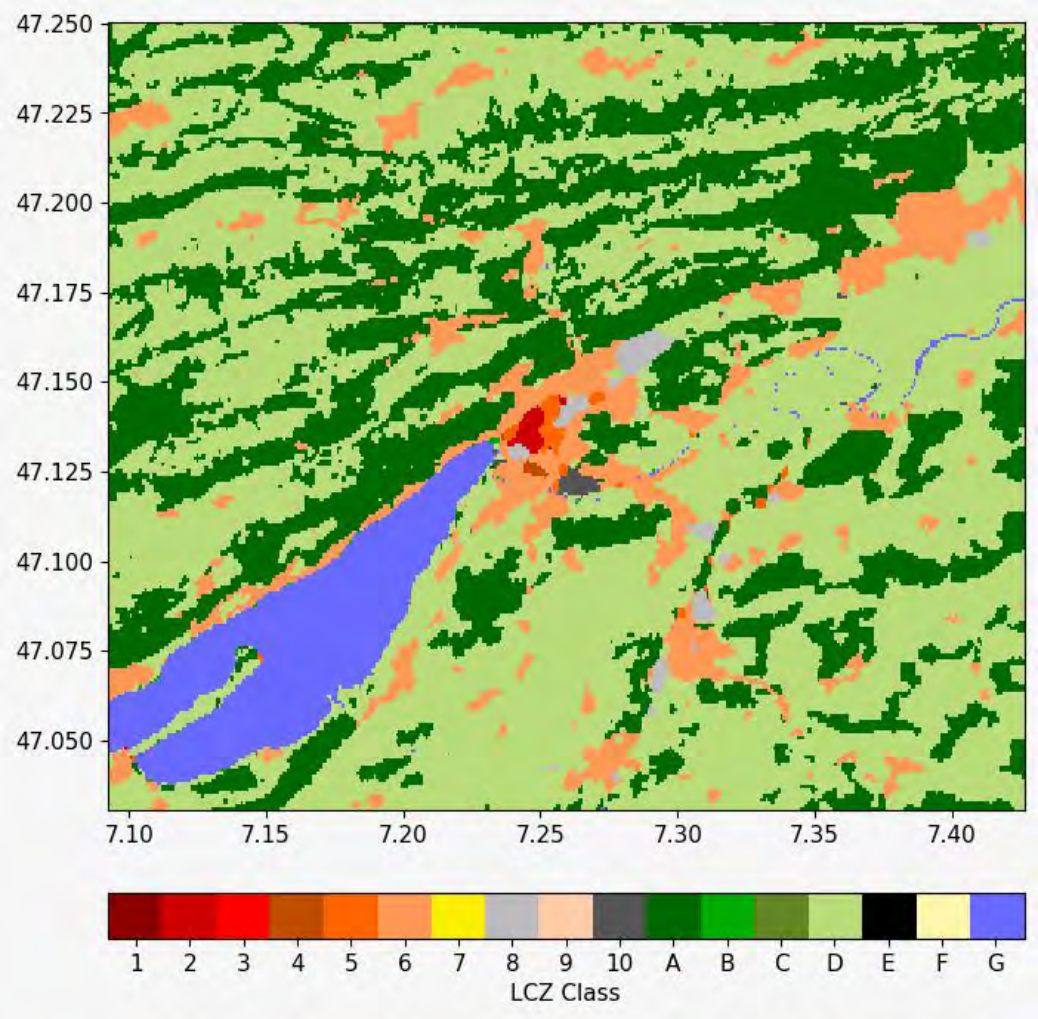

Figure 2.4: Local Climate Zone map of Biel generated through the Local Climate Zone Generator.

This study benefits from the temperature sensor network established in the neighboring city of Bern. A dense network of some 80 stations has been put up to measure air temperature (and some humidity stations as well) across Bern from May 15th to September 15th every year since 2018.[3] The results from Bern show the typical pattern of a UHI described previously: at most stations there is a minimum around solar noon and a maximum during the early hours of the morning (Gubler et al., 2021). This daily pattern is highly variable and dependent on both radiation bias from the sensor devices (more on this in the Methods and Discussion section) and due to local shading characteristics (Meyer et al., 2022). At night the city has UHI values that peak in the densest part of the city center, the old town, at about 5.5°C and descend to about 1°C in the suburbs (Gubler et al., 2021).

[3]The yearly data is freely available via the Boris database service provided by the University of Bern.

The results in Biel should show about the same pattern spatio-temporally, if less reduced due to the smaller size of Biel in general and especially of the dense, built up area around the central areas and the old town, compared to their counterparts in Bern.

Chapter 3

Methods and Data

This section will first describe the process to set-up the empirical sensor network, collect the data and matadeta, and the first steps of data processing. Select meteorological data from the nearest SwissMetNet stations during the summer will be shown as well. Next the Flow over Irregular Terrain with Natural and Anthropogenic Heat Sources (FITNAH) model will be reviewed and the process of buffering will be described. Finally the Spearman's *Rho* and Kendall's *Tau* measures of rank correlation used to compare the FITNAH model to the empirical data will be presented. All of the software packages and tools used to create this report are described in Annex 1.

3.1 The Sensor Network

The empirical network consists of 39 unique locations, each with one sensor.[1] There are 35 city locations, two forest locations, one rural reference site near the city and one reference located at the Grenchen SwissMetNet station. The in-situ sensor network follows closely the methodology employed by the GIUB in Bern and by the city of Zürich since 2018 (Gubler et al., 2021 and Meyer et al., 2022 and Burger, Suter, et al., 2024). The sensors are the same exact devices as those that have been used in Bern for the past five years, enclosed by the same radiation shields and affixed to lightpoles via the same mechanisms.

3.1.1 Description of the temperature sensors

The sensor device is composed of a battery-based temperature sensor enclosed within a radiation shield and affixed to its support with an L-bracket. In order to reduce costs, the radiation shield relies on passive ventilation for ensuring air flow, which comes at the price of increased measurement bias, particularly during periods of high incoming radiation (Gubler et al., 2021). The loggers have an accuracy of ±0.53 K between 0 and 50°C and a resolution of 0.14°C (Meyer et al., 2022). The sensors were affixed to lightpoles at a height of 3 meters, plus or minus a few centimeters of measurement error during the installation. The only exception is one forest sensor which is attached to a tree at a height of 1.5 meters above the ground. The placement of the sensors at three meters allows them to capture the dynamics of air temperature close to the surface where it matters to people's health and well-being but is still high enough to avoid deliberate or accidental damage (Gubler et al., 2021 and Organization, 2023). While air temperature measurements are often conducted at a height of two meters, the three meter height lies with WMO height guidelines for meteorological

[1] There is a duplicate forest sensor, sensor 240, at one location since the original sensor's radiation shield was damaged, presumably during a storm between early June and mid-July. This is assumed to not heavily impact the readings of sensor 214 based on a comparative analysis done on the time the sensors were concurrently installed. A chart is available in the annex. For the present analysis only sensor 214 is used.

measurements (Organization, 2023). The use of lightpoles provides a consistent structure on which to affix the sensors that is common throughout the city, providing flexibility in location choice and comparability within and between cities. A sticker in German was placed below the sensors explaining their purpose to further avoid vandalism and invite the public to learn more about the project.

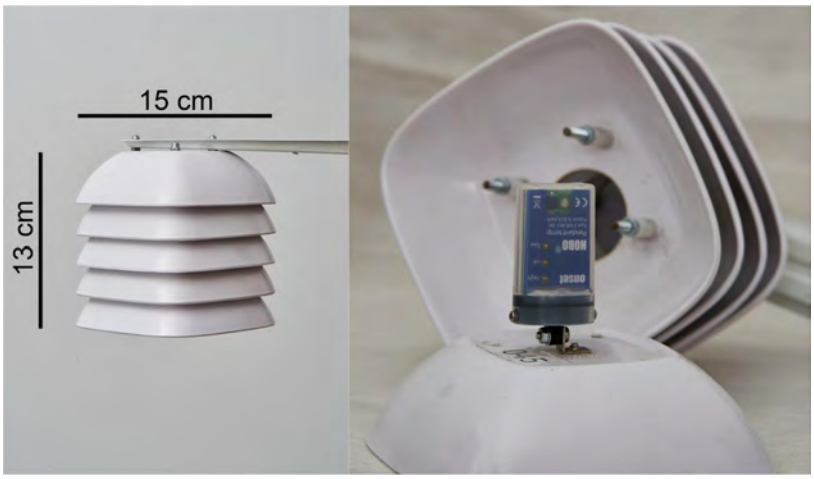

Figure 3.1: This image from Gubler et al., 2021 shows the sensor itself. The multilayered-white reflective shield is designed to reflect as much radiation as possible while providing for airflow. Such a system cannot, however prevent all radiation bias.

3.1.2 Data collection and Metadata

Air temperature data was collected at ten minute intervals to match the data collected by the Swiss national weather network and the Bern measurement network. The data is stored locally on the sensor, which can hold 42 days of data. Therefore, four data collections were organized in 2023 during the weeks of June 18th, July 28th, August 31st and September 25th (after the measurement period ended) in order to read the data out from the loggers onto a laptop computer. In 2022, two data collections were organized, first in the middle of the pilot period and the second at the end of the pilot period. In addition to reading the results, the research team cleaned the radiation shield and metadata was collected. Cleaning consisted of wiping the white radiation shields clean of debris that would reduce its effectiveness in reflecting radiation and dealing with insect nests and occupants inside the sensors. The latter was largely a problem of forest, rural, park and lakefront sensors. The attachment was checked to make sure that it still held firmly to the lightpole. The data collection was accomplished largely by your author, alone or accompanied by one person either from the environmental department of Biel/Bienne or the GIUB. During the first reading, GIUB students from the StadtKlima summer course collected most of the data and metadata during a two day period.

The metadata consists of three parts. First, the research team takes five photographs during sensor installation and at each read-out. This enables changes in the series to be potentially linked to physical changes in the environment. The photos consist of a picture of the station taken from several meters away at eye level and one picture in each cardinal direction at the height of the sensor. The second aspect of the metadata photos are the 'fish-eye' photographs taken from the top of the sensor skyward, which provide the ability to estimate the Sky View Factor (SVF), the proportion of atmosphere to which the station has an unobstructed view; this is the critical parameter governing longwave radiation escape described in the introduction (Oke et al., 2017). Finally, metadata sheets

record all relevant details about the station. This includes for example, the height of sensor attachment to the pole, the distance from the pole to the sensor, a description of the vegetation, notes about any changes, and a description of the lightpole itself. An example of the metadata sheets and the fish-eye photos are provided in the annex.

Figure 3.2: These photos document station 201 during the first reading on June 18th 2023. At each reading, these 4 sets of pictures were taken for each station. This station is an example of a location at a street junction, over a relatively uniform area, about equidistant from all buildings. This location was the area transformed from the General Motors auto factory into the COOP Shopping center visible in the top right image mentioned in chapter 2.**Top left:** South; **Top Right:** East; **Bottom left:** North; **Bottom right:** West

.

3.1.3 Determining sensor locations

The base of the Biel network came from the 2022 pilot project which used seven sensors from early July to mid September (sensors 201 - 207). The five urban sensors (201 - 205) were placed in a line along the Suze river from the Lake to near Bözingen which cuts through the center of the city. The decision needed to be made about how to allocate the remaining sensors. Zürich and Bern each took a different approach in designing their initial sensor networks in 2018 (Burger, Suter, et al., 2024). Zuerich opted for a high density grid approach of roughly 200 sensors, while Bern opted for an LCZ-driven approach of about 80 sensors. Since then, Zuerich has opted for a targeted approach as well, with 100 strategically placed sensors throughout the city (Burger, Suter, et al., 2024). Initially, this study followed the LCZ framework as well, but key features to be tracked were related to social and topographical aspects of the city, rather than land-use and building geometry.

Therefore the LCZ framework is used as a guide and check to the sensor locations, rather than as a principal determinant. The following points guided sensor placement of the 39 sensor locations.

Criteria for Sensor Placement
Identify general pattern of UHI across Biel and Nidau
Representation across the different neighborhoods
Representation of the Taubenloch Gorge
Representation of each Local Climate Zone
Inclusion of retirement homes and health facilities
Inclusion of green areas such as parks and forest
Inclusion of water areas such as river fronts
Coverage of previously studied urban climate phenomenon in Biel
Inclusion of the five 2022 pilot locations
Forest Sensors
One rural reference and one SwissMetNet reference
Use of pairwise sensors to evaluate the impact of different phenomenon
Identify the maximum UHI in the city and quantify it

Table 3.1: Criteria for Sensor Placement in the Biel sensor network

Figure 3.3: A satellite photo of the rural reference sensor 206 with the distance to the nearest house and the nearest cluster of houses marked, respectively about 40 and 200 meters away.

The rural reference location (206) was greatly constrained by the local topography and significant industrial, suburban and urban development in most directions, therefore the only suitable region was in the Orpund direction, Southeast of Biel. It was placed on a fence that separates a field undergoing a corn crop rotation in 2022 and 2023 as well as a vegetable and berry farm which maintains relatively homogenous crops over time. It is located roughly 40 meters from the nearest building (a farmer's house) and about 200 meters outside of the built agglomeration of Biel, as shown in Figure 3.3. The rural reference is located in a depression where the cold winds from the Jura are redirected away from the city, between the Vorholzli and the Längholz. The second reference sensor was located approximately 4 meters away from the two meter air temperature measurement

from the SwissMetNet Grenchen airport (GRE) station, 14 kilometers East of Biel. This allows the differences between the official measurement and the LCD sensors to be evaluated and bias to be addressed.

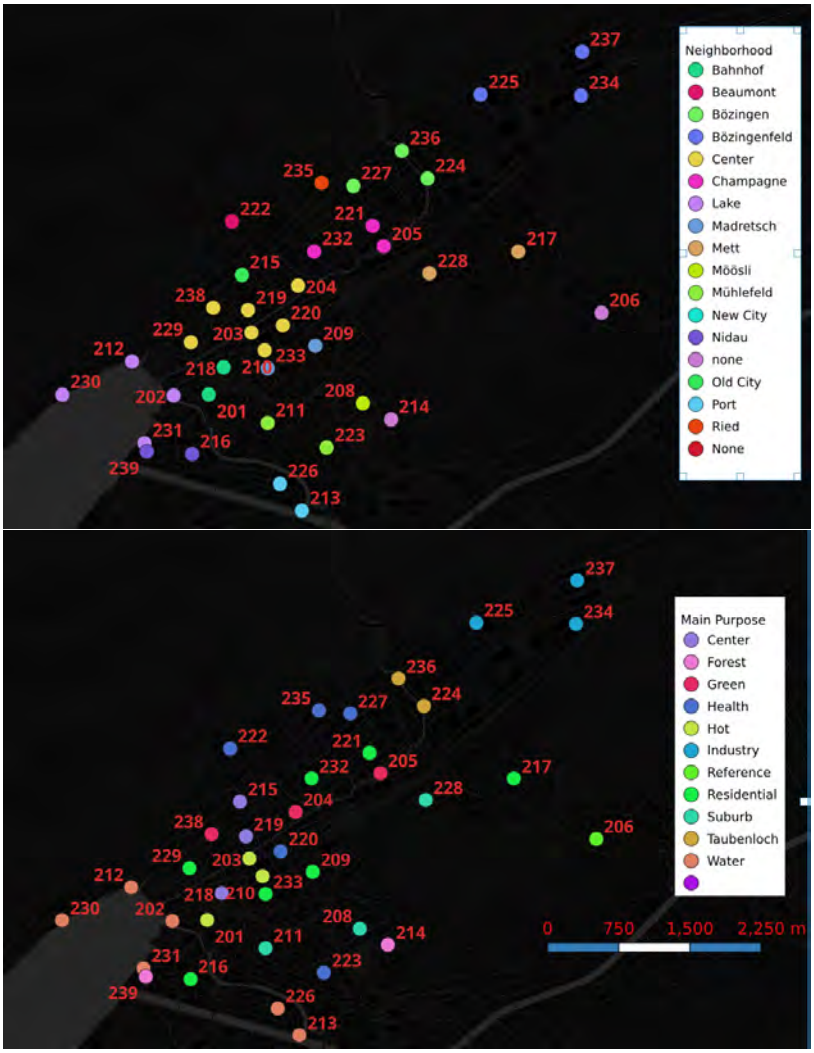

Figure 3.4: The top image shows the neighborhood of each sensor, while the bottom image shows the main feature / purpose of each sensor.

Many of the locations for the remaining sensors were somewhat fixed due to the above constraints, beginning with the decision to keep the same five pilot sensors. Capturing the effect of the water front areas committed four sensors to the lake front and the Nidau-Büren Kanal. Covering the cold air flow through the Taubenloch gorge constrained an additional two sensors. Five sensors were requested by the city authorities in Biel measure the impact of the UHI on four retirement homes and the hospital owned by the city. Two sensors were placed in forests. The center of the city was over represented in order to be sure to identify the maximum UHI of the city, as this would most likely occur in the central neighborhood due to its density and based on the location of the hot spots identifed in previous urban climate research in Biel (Wanner, 1991). The remaining sensors were distributed judiciously throughout the city based on capturing the geographic extent of the city and

the availability of suitable lightpoles to affix the sensors. The larger neighborhoods of Madretsch, Champagne, Mett, and Nidau-Port each received two sensors. Figure 3.4 shows the neighborhoods of each sensor and the purpose / major feature at that sensor's location. A table of sensors, their long names, neighborhood, and purpose is also available in the annex.

3.2 Temperature Sensor Data

In 2023, Of the 39 sensors placed, 35 have complete series from the beginning to the end of the study period and the remaining 4 sensors have partial data. This is summarized in the table below, with a more detailed description available in Annex one. In addition, each sensor has three periods of missing data: data was removed ten minutes before and one hour after each of the three data readings described above. There was no other treatment applied to the data.

Station	**Category**	**Issue Description**
231 (Vingelz Lake)	Water	Installed late (June 6th); Data contaminated during summer by heat from a food truck under the station.
214 (Längholz Forest)	Forest	Installed late (June 14th); Damaged radiation shield; logger 240 was added as a backup for the last 3 weeks.
239 (Nidau Forest)	Forest	Installed late (July 3rd)
230 (Nidau Lake)	Water	Late start (June 19th); Unkwnown interruption August 18th to August 31st, caused by unknown sensor failure.

Table 3.2: Summary of missing and irregular data issues for specific sensors.

3.3 Meteorological Data

Biel is located about equidistant from three meteorological stations on the Swiss Plateau: Grenchen, SO (15 kilometers), Cressier, NE (19 kilometers) and Zollikofen/Bern, BE (26 km). Cressier and Grenchen both lie at about the same elevation as Biel, while Bern is about 100 meters higher. The daily mean, maximum and minimum air temperatures are plotted on below for these three stations and the 207 reference sensor. There are three distinct periods of heat: July 08-12th, August 12th - 24th and September 08th - 13th shaded in blue. The August heatwave was the most severe in terms of maximum, mean, and minimum air temperatures, as well the longest in duration. The daily wind speed and humidity are both somewhat higher in Cressier and Grenchen, but overall these indicators are broadly comparable as can be seen below.

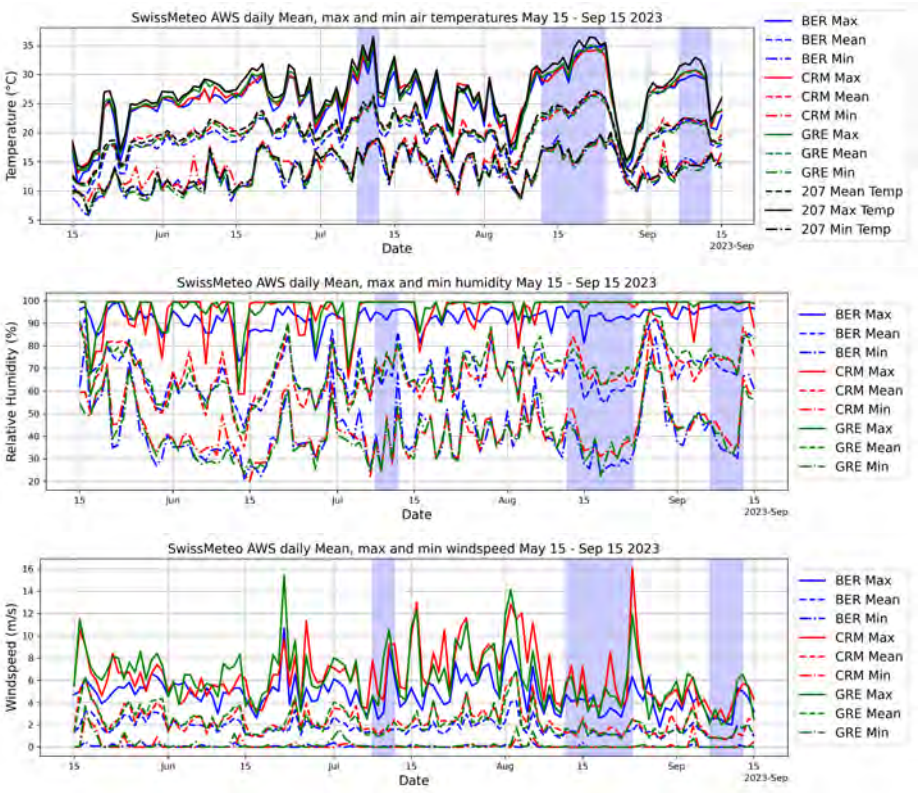

Figure 3.5: Plots of daily temperature, windspeed and humidity at the three closest meteorological stations. The reference sensor 207 is included in the temperature series.

3.4 The FITNAH Model

In summer 2023 the canton of Bern published the results of a study it commissioned on the UHI throughout the canton of Bern. The final result presented to users comes in the form of eight data files in geotiff format. A geodata layer for urban spaces and for urban streets is provided for projected UHI at two meters height at 14:00 and 04:00 for an 'ideal' day in 2020 and 2060. All areas that are not classified as urbanized or streets do not have UHI data. In addition to the publicly available output UHI layers, GeoNet provided the raster files that the analysis was based on to the GIUB, most importantly the land use files and a raw temperature layer that extends throughout the canton. The data layers used in this present work are the urban space and street data for 04:00 AM in 2020.

The model solves a series of physical and thermodynamic equations to model the flow of energy and mass through the urban system. The horizontal resolution is 10X10 meters, while the vertical resolution scales up from 4m, 10m, 15m, 20m, 30m and so on, gradually increasing the size of the increment until 3000 meters (Geonet, 2023b). At a height of 3000 meters it is assumed that land use no longer has an impact on air temperature and flow. The input layers consist of geodata provided by the relevant Swiss authorities: the 25 meter digital elevation model (DEM), the 10 meter resolution land use data, Swiss Buildings 3D height dataset, and the national vegetation height model. These datasets combined provide a relatively complete picture of the urban terrain at a reasonable resolution given the cantonal scope. GeoNet assigns climatic properties to raster cells using the various geospatial inputs for land use categories, elevation, building height and vegetation

height. A zonal statistical aggregation method is used to scale features and provide smoother inputs for the model.

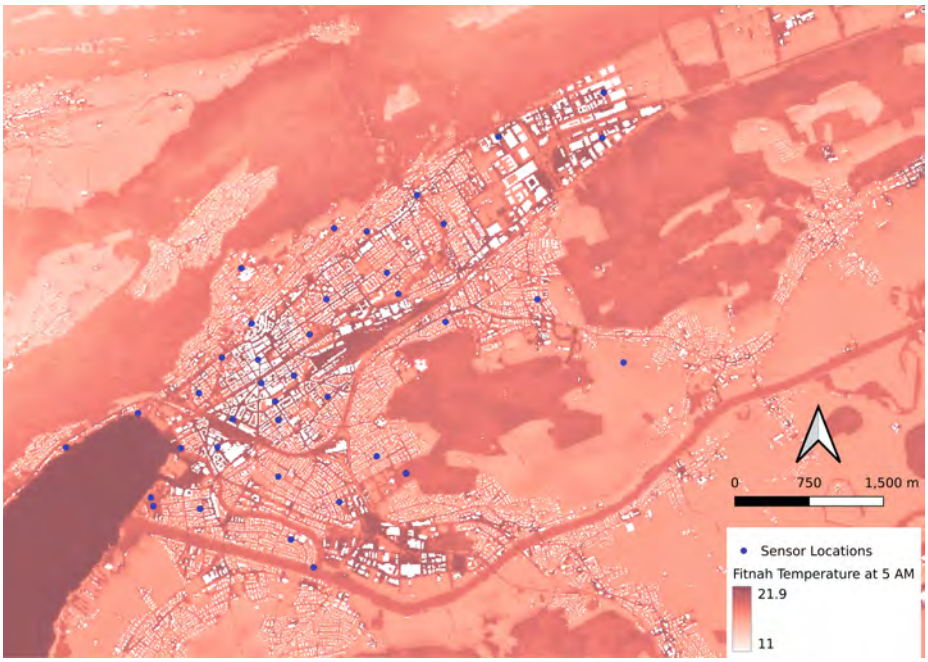

Figure 3.6: The FITNAH temperature layer around the city of Biel. The white indicates missing data and the blue dots are the sensor locations.

The model starts on an 'ideal' day with 50 percent relative humidity, no overlying geostrophic wind, and no cloud cover (Geonet, 2023b). This is inline with objective of modelling urban cooling processes under the "worst case scenario", which is a very hot day without large scale wind patterns to facilitate air exchange. The cooling of the city will therefore be dependent on local processes driven by local cold air flows and temperature gradients. This is the source of the name FITNAH, it focuses on production and flow of cold air in and around urban regions. The air temperature used as a rural reference appears to be the nearest SwissMeteo station at 21:00 combined with a geospatial model to extrapolate temperatures throughout the canton. The model begins at 21:00 on "June 20th 2020" and runs in one hour timesteps until after 14:00 the next day. Further information is not readily available from the report regarding the initial conditions or the running time of the model.

The FITNAH model data for the city of Biel is presented below. The general temperature layer is not available to the public, while the streets and spaces layers are the public facing ones. Each of these layers contains significantly less data than the overall temperature layer. The analysis will therefore make use of all three of the layers, but the results from the temperature layer should be the most robust thanks to the additional data points that are available in any given location.

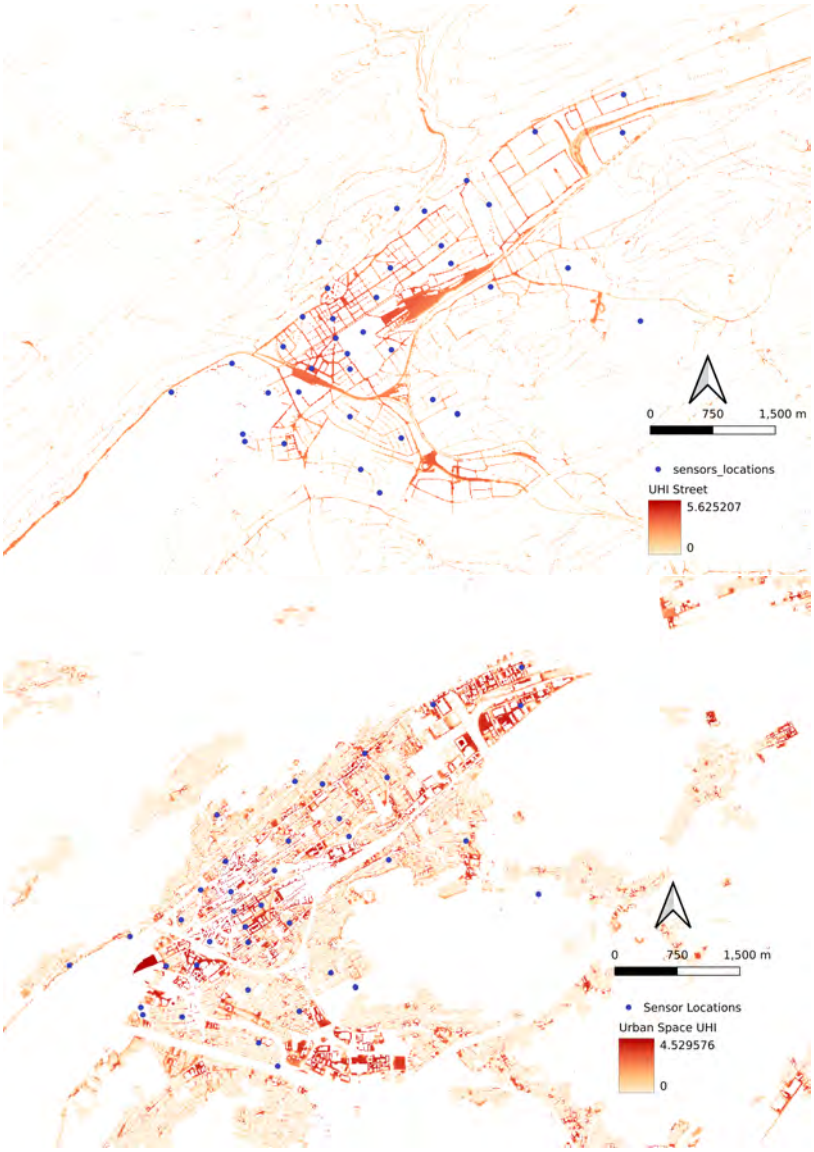

Figure 3.7: The top figure is the UHI Streets layer provided by geonet, which contains UHI values for all raster tiles considered street under the SwissTopo land use categories. The bottom figure is the UHI Spaces layer, which contains UHI values for all areas considered to be urban spaces. Both of these have substantially less data than the fitnah temperature layer.

Figure 3.8: Overview of the buffers used in making the dataset. The top left demonstrates the space taken up by buffers of 10, 50, 100, 500 and 1000 meters for station 203, Zentralplatz on the scale of the city. The same station has different characteristics based on the buffer chosen as can be seen in this representation. The top right image shows the central area with buffers of 10, 50 and 100 meters overlaying the FITNAH temperature layer. There is substantial amount of data at each station. The bottom left image shows the FITNAH space in Blue and the FITNAH street in red. There is substantially less data in both of these layers, even added together than in the FITNAH temperature layer. The bottom right image shows the area immediately to the West of station 204, the city park. Neither the pictured grass nor parking lot are show as either urban street or space data. The entire rest of the park to the East, North and South is also included only in the FITNAH temperature layer.

The data used to rank the FITNAH output and input layers was taken using circular buffer zones around each station ranging between five and 1000 meters. The FITNAH outputs and non-landuse inputs are summarized using the mean and the median. The landuse values are summed for each raster pixel encoded as that land user category in the buffer zone, since they are categorical. Figure 4.5 visualizes the process of buffering the data. The FITNAH output layers UHI Street and UHI Space have missing values or few values for low buffers, while the FITNAH temperature layer is complete throughout the city. The city parks in particular have missing data for both UHI space and UHI street.

3.5 Evaluation of the UHI and Heat Indicators in Biel

In addition to the UHI, the City Index, Tropical Nights and Hot Days are calculated for each station. The latter two indicators are commonly used in research and policy making, most notably by Swiss

Meteo MeteoSwiss, n.d. The City Index is used to compare the stations between each other and has proven useful for evaluating models Burger et al., 2022. Due to the sensor bias, Tropical Nights and Summer Days are calculated for several different thresholds to account for bias in the sensor data. The UHI and the City Index do not require this method as they are based on comparisons between the sensor network. The City Index is also calcuated for the FITNAH temperature model and used to look at the differences in heat distribution predicted by the model and measured by the empirical network.

Definitions for Key Metrics
Tropical Night: The station's minimum temperature exceeds 20°C
Hot Day: The station's maximum temperature exceeds 30°C on that day
UHI: The difference between the urban station and the rural reference
City Index: The difference between the temperature of that station and the mean temperature of all stations in the measurement network

Table 3.3: Definitions of Key Metrics

These indices are calculated for the main summer heatwave period from August 12th to August 24th, 2023 and for the entire study period from May 15th - September 15th 2023. Studying the heatwave period in isolation is important because the UHI is most intense during clear, summer days and nights (Oke et al., 2017). In addition, the health risks related to the UHI and the temperature distribution of the city are most acute during such periods and therefore merit study. The overall period is also used to provide a general outlook on the UHI at each station. During the heatwave period, only one sensor is missing data (230), which has partial data during this period. For the cumulative tropical nights and summer days, it is not clear that the other stations (239, 230, 231) would be severely affected since the majority of the both of these indicators occur after the data interruption period.

3.6 Identification of cold air flows

The cold air flows identified in the previous urban climate research on Biel should be visible as a drop in temperature relative to other stations. In particular, the appearance of the Taubenlochwind bringing air from the Valley of St. Imier should be clearly visible as it moves a large amount of cold air from a nearby peak (the Chasseral) (Wanner, 1991). The onset of katabatic winds bringing cold air down the mountain slope could also be visible in sensors on the Northern edge of the city. Both of these should peak in the first half of the night as described in previous research in Biel (Wanner, 1991). The approach taken is to examine the boxplots of hourly city index of stations that are likely to be affected and compare them to those that are not.

The stations used are divided into comparison stations, strong Taubenloch stations, weak Taubenloch stations, and katabatic wind stations. The comparison stations are in the middle and Southwestern part of the city well away from anticipated effect of these winds. The strong Taubenloch wind stations are located directly at the mouth of the gorge and approximately 300 meters directly South. The weak Taubenloch wind stations are those around these two stations, where a diversion of the wind could cause the effect to be visible.

Station Groupings by Characteristics
Comparison stations: Station 203, 201, 209, 208
Strong Taubenloch wind: Stations 224, 236
Weak Taubenloch wind: Stations 205, 221, 225, 227, 228
Katabatic winds: Station 212, 215, 222, 225, 227, 235, 237

Table 3.4: Station Groupings Based on Wind and Comparison Criteria

3.7 Comparison of model and empirical data

Since the period that is calibrated in the model is June 2020 and the empirical data comes from 2023, it is not possible to do a direct comparison between model output and empirical data as was done in (Burger et al., 2022). Instead, the sensor locations will be ranked according to the magnitude of the UHI and the city index in the early morning at 4 am during (a) The whole period May 15 - September 25 2023 and (b) the August Heatwave Aug 12 - August 24 2023. The FITNAH data is ranked according to the temperature layer and the UHI layers provided by Geonet. The landuse raster data is ranked by the sum of each pixel of a given land-use feature within a given buffer.

The correlation between the rankings from the UHI, temperature and land use around each station are each tested using Spearman's Rho (SR) and Kendall's Tau (KT). These are similar measures of the ordinal comparison between two sets of data, which share the fundamental assumption that there is a monotonic relationship between the datasets under consideration (Puka, 2011) Each of these methods are robust to non-normal data and small sample sizes, and is therefore used to measure the strength of monotonic relationships in environmental data (Rinner and Hussain, 2011, Fan and Wang, 2020, Elmarakby and Elkadi, 2024). In order to apply SR and KT, the two comparison datasets are ordered by magnitude from 1 to n, where n represents the number of observations to be compared. Both SR and KT range from -1 to 1 and the sign indicates whether the relationship is negative or positive. The magnitude of the relationship is indicated by the size of coefficient: values closer to 0 indicate a weak relationship and values closer to 1 or -1 indicate a strongly positive or weak relationships. Both SR and KT are calculated using the *scipy.stats.spearmanr* and *scipy.stats.kendalltau* Python packages respectively (Virtanen et al., 2020).

$$r_s = \rho_{R(X),R(Y)} = \frac{\mathrm{cov}(R(X), R(Y))}{\sigma_{R(X)}\sigma_{R(Y)}} \tag{3.1}$$

where $\rho = \dfrac{cov(X,Y)}{\sigma_X \sigma_Y}$ is the Pearson correlation coefficient applied to the rank variables, $\mathrm{cov}(R(X), R(Y))$ is the covariance of the rank variables, and $\sigma_{R(X)}$ and $\sigma_{R(Y)}$ are the standard deviations of the rank variables.

For the KT metric the procedure is to compare, for all pairs of data points in the two samples the following: If I draw (x_i, y_i) and then I draw (x_j, y_j), and if $x_i < x_j$ then the pair is concordant. If $y_i < y_j$) then the pair is discordant. The total number of concordant and discordant pairs are summed into C and D, respectively. The Kendall's Tau-b method shown and used here adjusts for instances of tied data. This adjustment weights by the number of ties that occur in the x series but not in the y series, given by X_0 and vice-versa (Puka, 2011).

$$\tau_b = \frac{C - D}{\sqrt{(C + D + X_0)(C + D + Y_0)}} \tag{3.2}$$

Chapter 4

Results

This chapter presents the results of the study. First the reference sensors are compared to data from the nearest SwissMetNet stations. Second, the distributions of the heat indicators are mapped out and overall results are shown. Third, the results of the empirical network and the FITNAH model data are compared.

4.1 Comparison to SwissMeteo and Bias Calculation

The performance of the rural reference sensor 206 and SwissMetNet reference sensor 207 compared to the results of the three nearest SwissMetNet stations is presented in Table 4.1. Both sensors 206 and 207 have higher mean, variance, and maximum temperatures than SwissMetNet GRE in both years. Both sensors 206 and 207 show extra summer days compared to GRE and the other two SwissMetNet stations. There is one extra tropical night in 2023 for station 207. Overall, the SwissMetNet stations are comparable among themselves for both periods.

Station (2022)	**Mean (°C)**	**Min (°C)**	**Max (°C)**	**T. Nights**	**S. Days**
Zollikoffen, BE	20.1	9.3	35.1	0	8
Cressier, NE	21.5	11.2	35.0	0	12
Grenchen, SO	20.7	9.8	36.0	0	10
Rural Ref 206	21.4	10.2	36.3	0	19
AWS Ref 207	21.3	10.8	36.9	0	21
Station (2023)	**Mean (°C)**	**Min (°C)**	**Max (°C)**	**T. Nights**	**S. Days**
Zollikoffen, BE	19.3	5.8	35.1	0	14
Cressier, NE	20.1	8.2	35.4	0	19
Grenchen, SO	19.7	6	35.6	0	27
Rural Ref 206	20.4	7.3	36.7	0	34
AWS Ref 207	20.3	6.4	36.5	1	35

Table 4.1: Comparison of loggers 206 and 207 with the three nearest SwissMetNet stations for 2022 and 2023. The table summarizes mean, minimum, and maximum temperatures, as well as the number of tropical nights and summer days recorded at each station. Both loggers 206 and 207 consistently recorded higher temperatures and more summer days compared to the SwissMetNet stations. Notably, logger 207 was the only station to record a tropical night in 2023. The data for 2022 covers the period from July 9 to September 14, while the 2023 data spans May 15 to September 15.

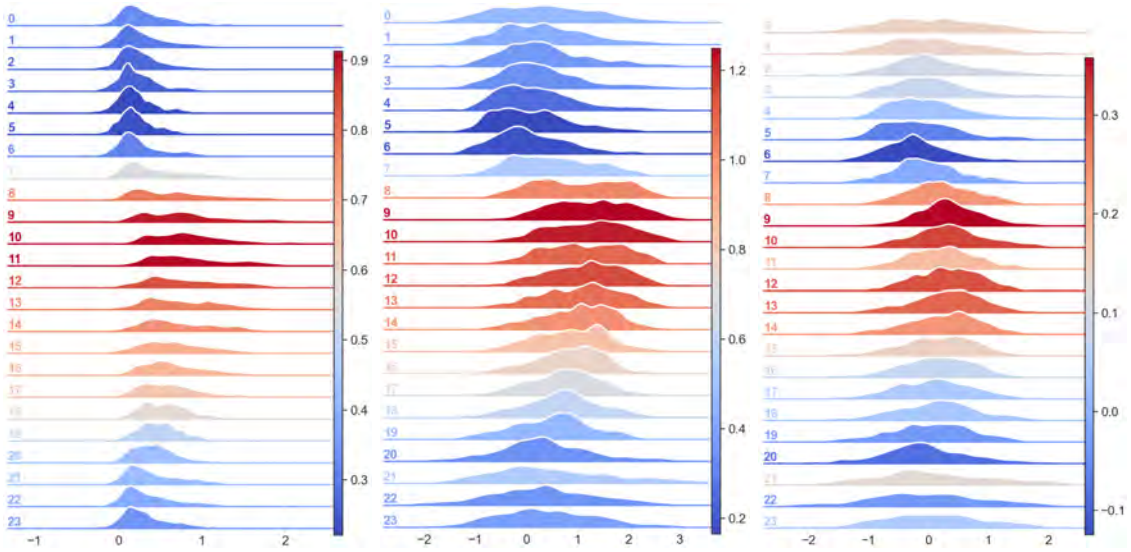

(a) 207 vs. GRE (b) 206 vs. GRE (c) 206 vs. 207

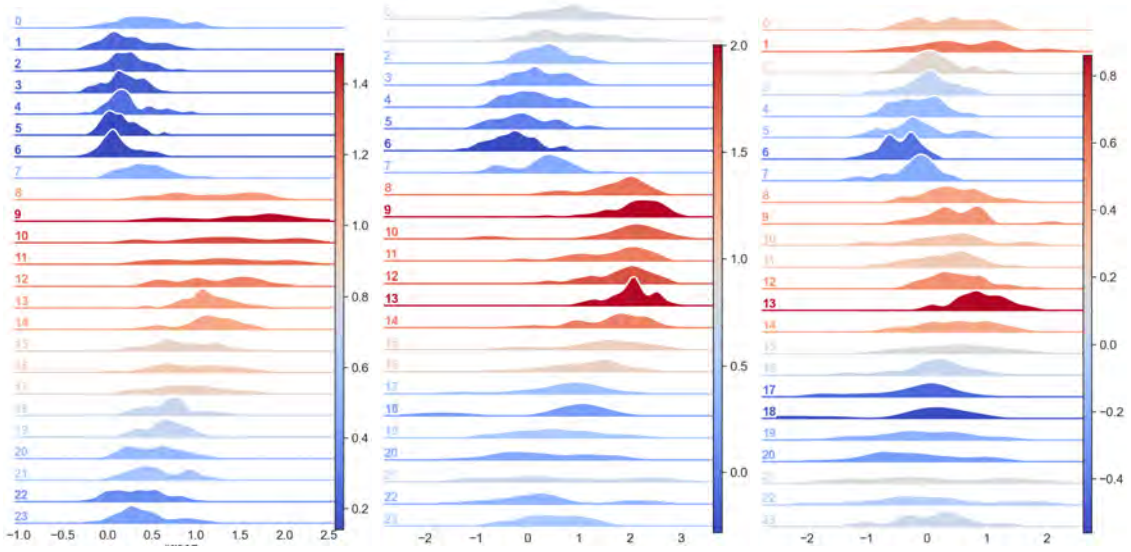

(d) 207 vs. GRE (heatwave) (e) 206 vs. GRE (heatwave) (f) 206 vs. 207 (heatwave)

Figure 4.1: Comparison of hourly temperature differences using ridge plots. The top row represents the entire study period, while the bottom row represents the summer heatwave. Each plot displays the hourly temperature difference, with the y-axis representing hours, the x-axis showing the temperature difference (°C), and the color indicating the mean temperature difference for that hour.

The higher temperatures recorded at the LCD stations compared to the meteo stations are mainly due to a radiation bias that occurs during the middle of the day. As shown in the ridge plots in figure .1, the bias falls to between 0 and 0.5°C at night, and rises to above 1°C during the daytime. This pattern is more pronounced during the heatwave period. The difference between stations 206 and 207 is relatively low during both summer 2023 and the August heatwave. Another view of the bias is provided in Annex 1 using boxplots.

Number	Location	UHI 04	UHI 12	UHI 20	T. Nights	Excess S. Days
201	Robert-Walser-Platz	2.76 ± 1.27	-0.19 ± 0.95	1.21 ± 0.99	10	-7
202	Hafen	2.52 ± 1.18	-0.28 ± 1.47	1.02 ± 0.84	10	0
203	Zentralplatz	3.32 ± 1.48	-0.58 ± 0.95	1.83 ± 0.97	14	3
204	Stadtpark	1.89 ± 1.16	-0.13 ± 0.97	0.64 ± 0.72	4	9
205	Ile de la Suze	1.85 ± 1.53	0.74 ± 0.82	0.47 ± 0.67	3	4
206	rural reference	0.0 ± 0.0	0.0 ± 0.0	0.0 ± 0.0	0	0
207	Swiss Meteo Reference	-0.03 ± 0.84	-0.31 ± 0.62	0.08 ± 0.95	0	-1
208	Möösli	1.41 ± 1.0	-0.03 ± 0.57	0.73 ± 0.65	2	4
209	Madrestch-Piano	2.89 ± 1.63	0.1 ± 0.88	1.25 ± 0.86	11	-6
210	Congresshaus	2.83 ± 1.36	-0.34 ± 0.82	1.34 ± 0.95	12	-4
211	Mühlefeld	2.19 ± 1.44	0.3 ± 0.79	1.14 ± 0.81	8	2
212	Seepark	1.96 ± 1.08	-1.16 ± 1.41	0.21 ± 1.03	5	-4
213	Port NBK	1.46 ± 0.94	-0.38 ± 0.81	0.78 ± 0.73	2	0
214	Längholz	1.33 ± 1.2	-1.65 ± 0.83	0.03 ± 0.76	3	-2
215	Old City	2.83 ± 1.47	-0.4 ± 1.11	0.68 ± 0.89	11	-7
216	Nidau-mittestrasse	2.36 ± 1.13	0.3 ± 0.88	1.0 ± 0.85	10	4
217	Geyisreid	1.4 ± 1.0	0.17 ± 0.62	0.72 ± 0.62	3	6
218	Bahnhof	3.23 ± 1.43	0.18 ± 0.95	1.91 ± 1.05	14	3
219	New City	3.44 ± 1.71	-0.01 ± 0.89	1.4 ± 1.0	15	5
220	Altersheim-Neumarkt	3.03 ± 1.43	-0.27 ± 0.65	1.53 ± 0.97	13	-6
221	Champagne-Piano	2.33 ± 1.37	0.11 ± 0.73	0.93 ± 0.78	10	8
222	Spital	2.12 ± 1.66	-0.53 ± 0.7	-0.31 ± 1.01	7	-5
223	Altersheim-erlacher	2.18 ± 1.14	0.05 ± 0.62	1.2 ± 0.84	9	10
224	Bözingen	1.96 ± 1.31	0.13 ± 0.59	0.26 ± 0.69	5	-5
225	Swisstennis	1.64 ± 1.1	0.37 ± 0.61	0.69 ± 0.92	6	0
226	Port Thielle	1.97 ± 0.99	0.15 ± 0.69	1.3 ± 0.79	8	4
227	Altersheim-redenweg	2.19 ± 1.5	0.62 ± 0.75	0.15 ± 0.93	7	2
228	Südstrasse	1.94 ± 1.36	0.03 ± 0.57	0.76 ± 0.61	5	5
229	Viaductstrasse	2.51 ± 1.23	-0.38 ± 1.27	0.78 ± 0.88	10	0
230	Vingelz	2.37 ± 1.18	-0.76 ± 1.05	0.34 ± 1.08	2	-15
231	Nidau-Lac	3.37 ± 2.92	-1.83 ± 2.62	0.72 ± 2.08	21	-13
232	Champagne-Blumen	2.62 ± 1.46	0.74 ± 0.66	0.94 ± 0.84	11	11
233	Madretsch-Zukunft	2.79 ± 1.56	0.51 ± 0.8	1.25 ± 0.89	11	3
234	Bözingenfeld	0.83 ± 0.96	0.24 ± 0.62	0.62 ± 0.68	1	3
235	Altersheim-Reid	1.78 ± 1.62	-0.76 ± 0.68	-0.57 ± 1.0	4	-6
236	Taubenloch	1.45 ± 1.36	-0.35 ± 0.85	-1.46 ± 1.5	3	-5
237	Rolex	1.26 ± 1.01	0.4 ± 0.82	0.75 ± 0.86	3	4
238	Museum	2.5 ± 1.56	-1.46 ± 1.17	0.36 ± 0.93	8	-15
239	Nidau-wald	2.2 ± 1.08	-2.71 ± 1.68	-0.25 ± 1.05	8	-20

Table 4.2: Overview of Results for the UHI network in 2023. The UHI 04, UHI 12, and UHI 20 columns contain the mean UHI at that hour plus or minus the standard deviation during the entire study period. T. Nights is the total number of tropical nights and Excess S. Days is the number of summer days at that station minus the number of summer days at station 206. Note that sensor 214, 230, 231 and 239do not have full data for the entire period and so the excess tropical nights/ summer days for these stations is skewed.

4.2 UHI, Summer Days and Tropical Nights in Biel

This section presents the results of calculating the UHI, the number of summer days and the number of tropical nights in Biel.

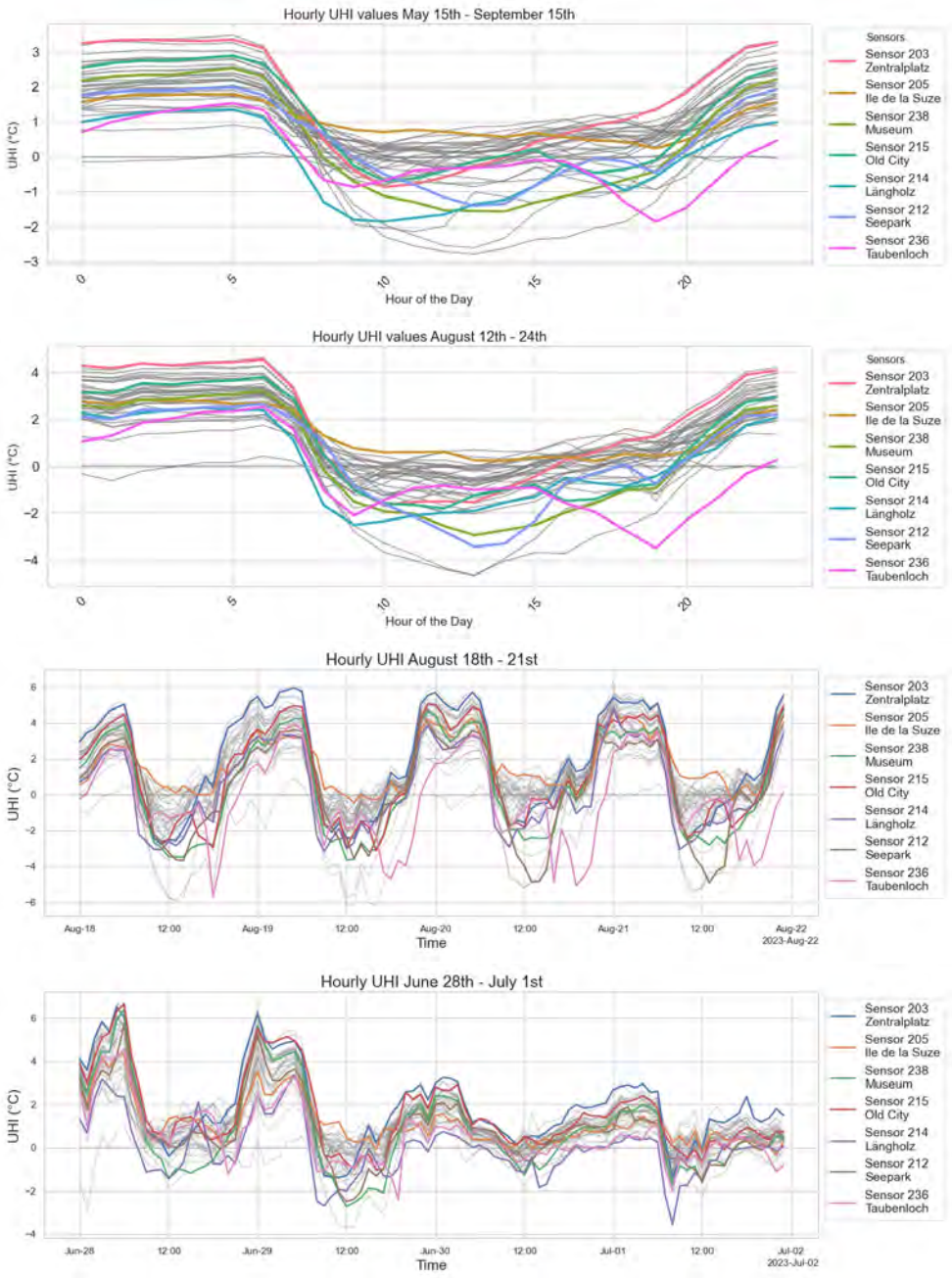

Figure 4.2: The hourly mean UHI for each station is shown in the first two plots above. The selected stations highlight key features of Biel. The bottom two plots show the UHI resampled to hourly means during a period of the summer heatwave and during a rain event earlier in the study period.

Figure 4.3: The mean heatwave UHI at different hours is on the left and the mean summer UHI at different hours is on the right. The first row is 4AM, the second row is 12PM, and the third row is 8PM. Notice the legends are unique to each plot.

The UHI results for all stations in the city over the study period (15-05-2023 - 15-09-2023) and during the August 2023 heatwave (12-08-2023 - 24-08-2023) are presented graphically in Figure 4.2 and 4.3. In Figure 4.2 we can see that the UHI for all stations exhibits a classic U-shape, which is most intense in the densest areas of the city. Illustrative of this is Zentralplatz (203), which lies is in the middle of the most built-up area of Biel and competes for the highest UHI, before falling down

to a negative UHI in the first half ot he day. The mean UHI is higher during the heatwave period than during the overall study period. During rain events, the magnitude and daily shape of the UHI changes, as represented by the bottom plot in Figure 5.2. At Zentralplatz, the UHI falls from 6°C to 2°C during an extended period of overcast and rainy weather. The effect of the Taubenloch wind is clearly visible at the Taubenloch through the sharp drop in UHI around 5 PM, but this effect dissapears during the rain event on June 30th - July 1st. Three noticeably cool stations during the day are Museum (238), the lake park (212) and Nidau lake (pictured in gray, and not included on the legend). On the other hand, the Ile de la Suze park (205) is relatively warm during the day and during the night.

These same results are shown spatially in Figure 4.3. The peak UHI at 4AM shows an inner circle at stations 218, 219, 210, 203 and 220, which tops out at above 3°C, and tapers off with distance away from this central region. The highest UHI at noon is around 1.5°C in the Champagne neighborhood (stations 205, 232) and away from the lake front. At 8 PM. the distribution is a bit more complicated with some of the lake stations warming up relatively, and Zentralplatz again heating up quickly relative to the other stations. The Taubenloch wind effect is clearly visible at this time. The katabatic winds that carry cold air down the mountainside could also be visible at 8 PM, as illustrated by station 235 and station 222.

The distribution of tropical nights and excess summer days for each station over the summer period is shown in Figure 4.4 The number of tropical nights is highest in the central part of the city, Madretsch and Champagne. It declines as the location moves further to the edge of the city. The effect of the lake is not pronounced on recorded tropical nights - for example there are fewer tropical nights in the Bözingenfeld industrial zone than at the lake front. The impact of the Taubenlochwind is again clear as station 236 has fewer tropical nights than all three of its neighbors. Notable as well is that the Bözingenfeld industrial area has few tropical nights.

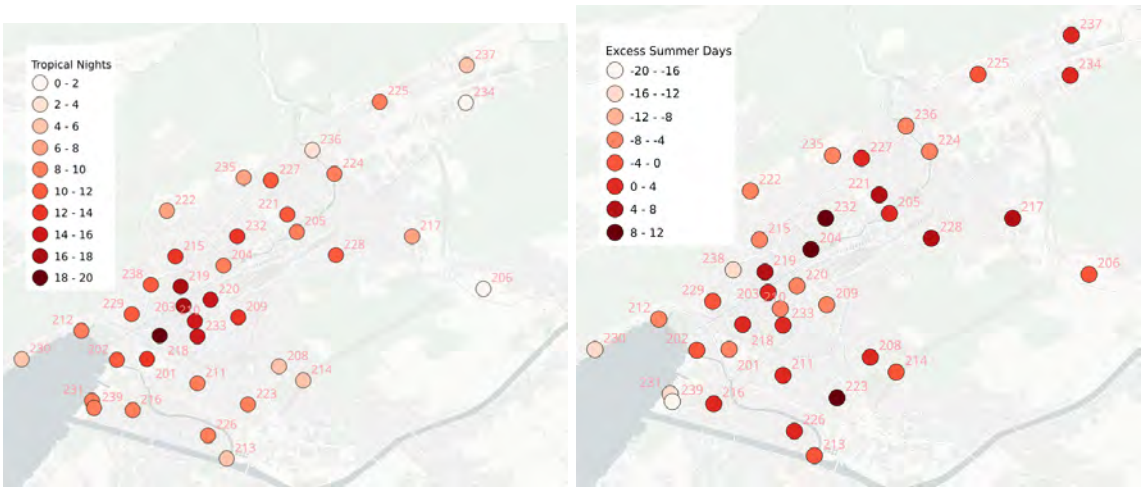

Figure 4.4: The Spatial distribution of tropical nights and excess summer days is shown on the left and right respectively. The excess summer days is calculated as the total number of summer days at each station minus the number of summer days at the rural reference sensor. The threshold uses is 31°C due to the sensor bias descibred in section one of this chapter.

The highest number of summer days occurs in the central Champagne neighborhood, in Bözingenfeld, and in the South of the city at one of the retirement homes. Like tropical nights, the overall distribution of summer days is affected by the lake, but the magnitude does not appear to be as large as might have been expected. One exception, the Nidau Forest, has very few summer days due to its location and due to the fact that it was not installed until early July, therefore the results should be

interpreted with caution. While few summer days were accumulated prior to July in most stations, it is possible that this station is not directly comparable to the other sensors. As shown in Figure 4.4, it is comparable in terms of tropical nights since few tropical nights were accumulated until after this sensor was installed, while summer days were recorded at other sensors before early July.

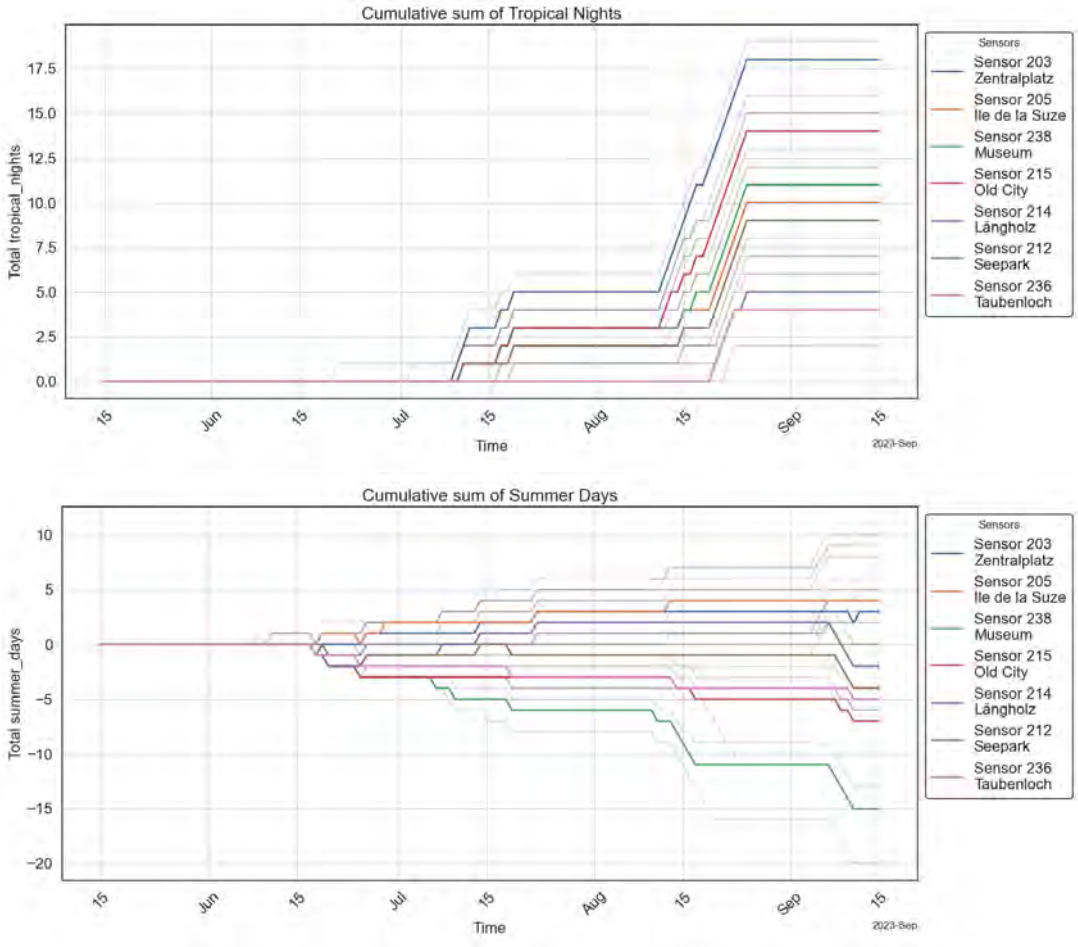

Figure 4.5: The cumulative sum of tropical nights (top) and summer days (bottom) at each station shows that both of these indicators increased primarily around the two heatwave periods in early-mid July and mid-late August.

At all stations, all of their tropical nights were accumulated during the two heatwaves, in July and in August. This can be seen in Figure 4.5, which shows the cumulative sum of tropical nights and summer days over the study period. Outside of these periods of heatwaves the cumulative sum does not change for most stations. The pattern is similar but not as distinct for summer days. These heatwave periods are visible as sharp increases in the cumulative sum, but there are summer days that are accumulative outside of the heatwave periods. Figure 4.6 shows how the amount of tropical nights and summer days at all stations would change if the threshold was incrementally raised. This shows that while these results are somewhat sensitive to bias and threshold selection, the results do not shift drastically in magnitude when the tropical night threshold is increased from 20 to 21. Similarly for summer days, the results are locally robust to small changes in the definition of the thresholds.

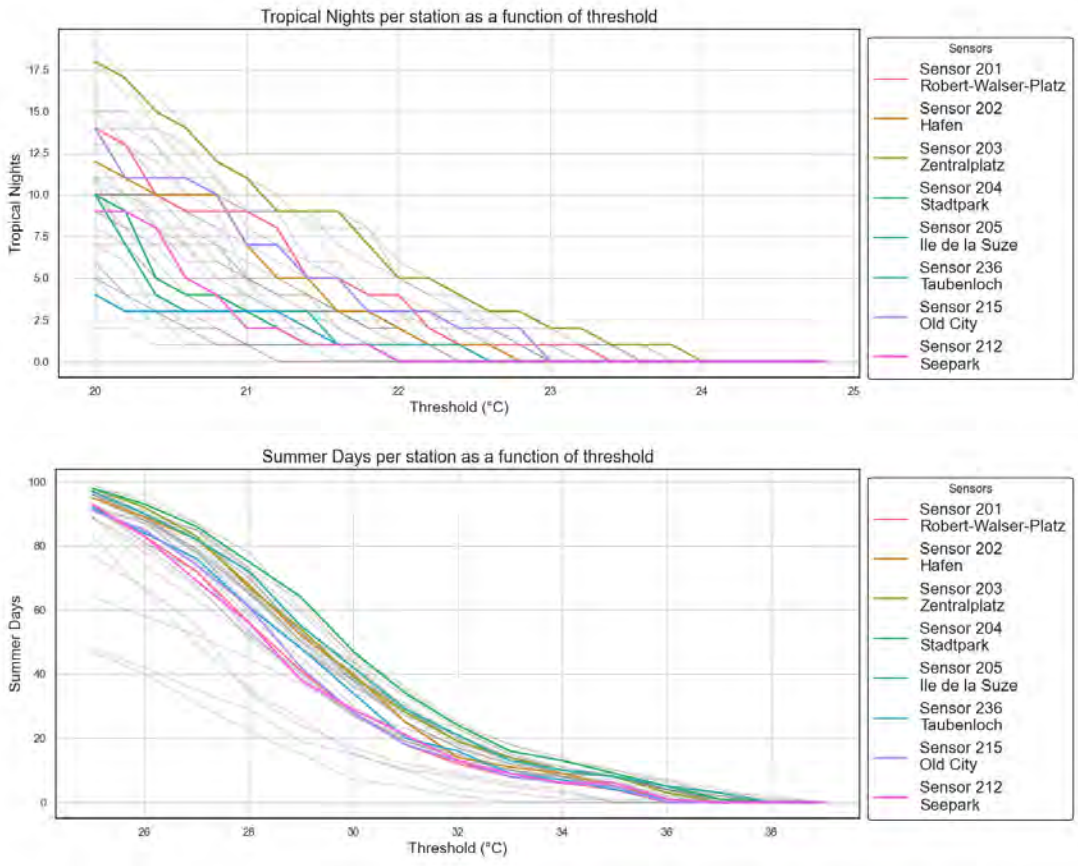

Figure 4.6: As the threshold to calculate tropical nights increases from 20°C, the number of tropical nights at each station goes down quickly. The same for increasing the summer day threshold from 30°C. The results presented use a threshold of 20°C for Tropical Nights and 31°C for Summer Days to account partially for the daytime bias.

4.3 Cold Air Infiltration

The first source of cold air into the city is the flow of the Taubenloch wind which should be detected by sensor 236 and sensor 224. The second main source of cold wind should be visible at the Northern edge of the city. Both of these should occur most strongly in the late afternoon and early evening, according to previous research (Wanner, 1991). The comparison sensors in Figure 4.7 show different patterns in the evolution of the city index that should be unaffected by this cold air flow. They all show a steady continuation of the trend in the period 17h00 - 23:00. Station 201, 203 and 209 are located in the dense, flat area of Biel. They show differing effects of shade and building configuration on the evolution of the UHI throughout the day and then consistently trends upwards from the early afternoon onwards. Station 208 is located on the backside of the Vorhölzli and trends downward relative to the other stations as the early evening passes. This station in particular should give pause to over-interpretation of the results presented later as such dips in the City Index are presumed to be a potential indicator of the impact of the cold air flow. The results from the August heatwave are used as this is the time when relief from high temperatures is most important and it is also when the effect should be most visible.

The results for any of the stations examined for cold air infiltration are most clear for the

Taubenloch wind at the Taubenloch station (236). Between 17:00 and 21:00 there is sustained cold air flow which reduces the city index to up to -5°C relative to other areas of the city. Stations 205 and 221 show a strong drop at 20h00, indicating that there could be some influence of cold air from the Taubenloch wind. Station 224, located most directly in front of 236, shows a sustained drop in city index from 18h00 - 21h00, perhaps indicating the influence of the Taubenlochwind as well. Station 228, located the furthest away but in the path of the Taubenlochwind also shows a drop at around 20h00. Sensor 225, located about 1 kilometer to the West at the base of the Bözingberg, does not appear to show any effect of either winds descending from Bözingenberg or the Taubenlochwind. Overall, the Bözingenberg katabatic winds appear to have some cooling effect visible in the city through the box plots, but outside of the moth of the Taubenlcoh gorge itself, the effect appears to be very slight, on average during the August heatwave.

The winds descending from the Beaumont are shown in Figure 5.9. Station 222 located on the mountain shows a sharp drop at 19h00, which is similar in timing to the Taubenloch wind. The stations that less than 100 meters away from the mountain, 238, 215, and 212, do not show a strong effect: for station 238 and 215 the upward trend appears unchanged, while for station 212, there is a slight drop at 1900 and 20h00. Stations 229, 219 and 232 are located 180 - 300 meters away and again show different patterns. Station 232 declines precipitously from 17h00 to 19h00 then grows steadily, station 219 shows a drop between 17h00 and 18h00. The fact that the trend is more visible in stations further from the mountainslope indicates that these drops may be artefacts of other influences and do not relate to the katabatic wind flow.

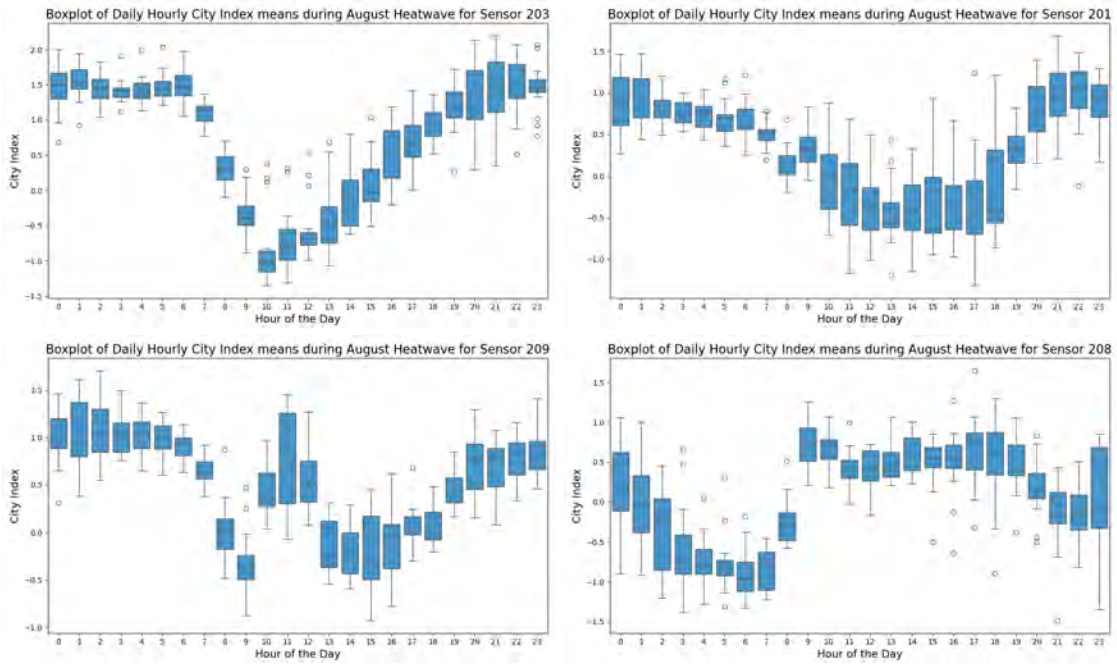

Figure 4.7: Hourly boxplots of mean City Index for sensors that are unaffected by the cold wind infiltration of the city from the Northern mountains or from the Taubenloch Gorge. They offer a comparison to the next set of plots.

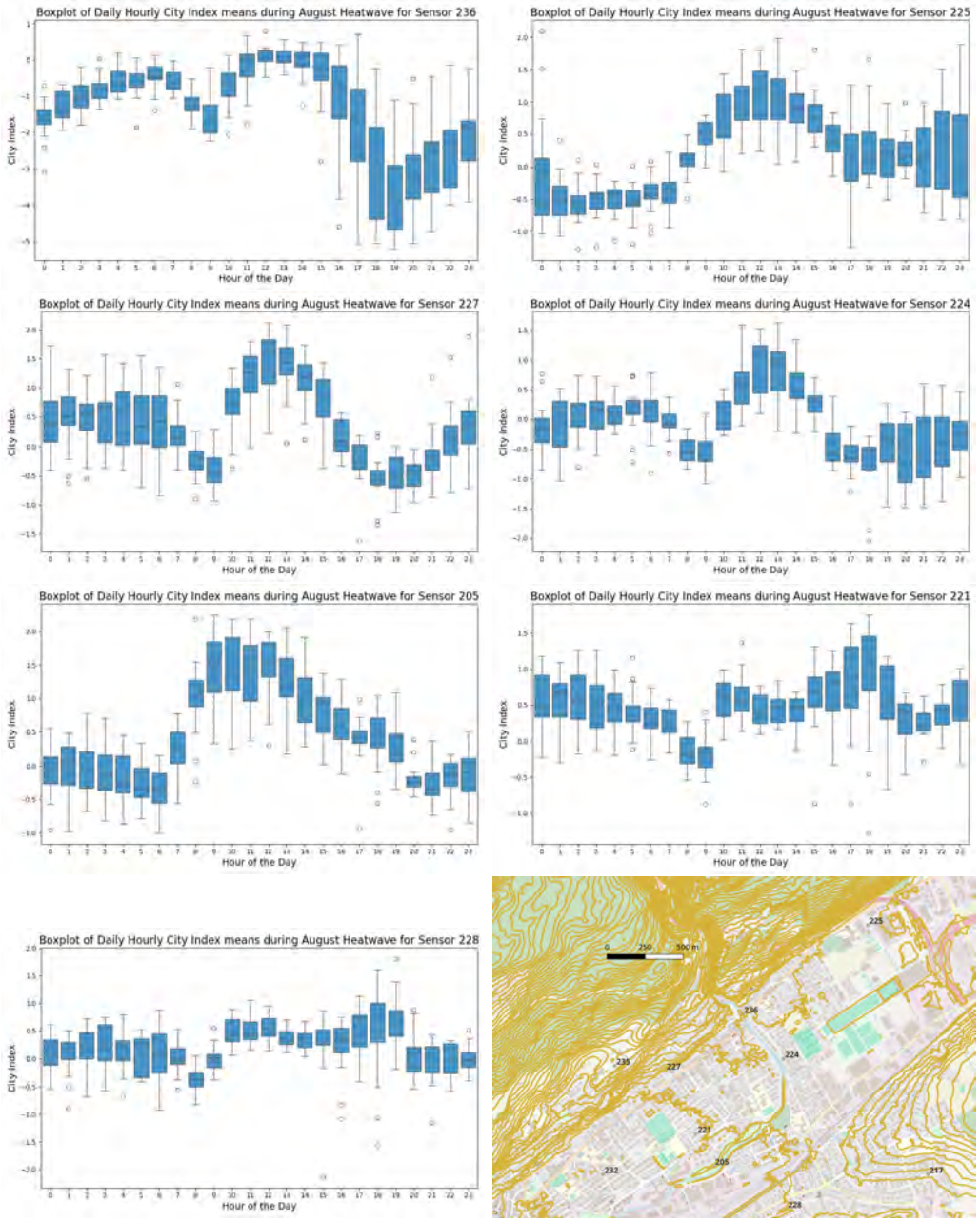

Figure 4.8: Hourly boxplots of mean City Index for the sensors located near the Taubenloch gorge. Station 236 is at the mouth of the Gorge and sTation 227 is 500 meters directly West, station 225 is 1000 meters East, station 224 is 380 meters South, and station 221 and 205 are about 800 and 100 meters to the South West, respectively.)

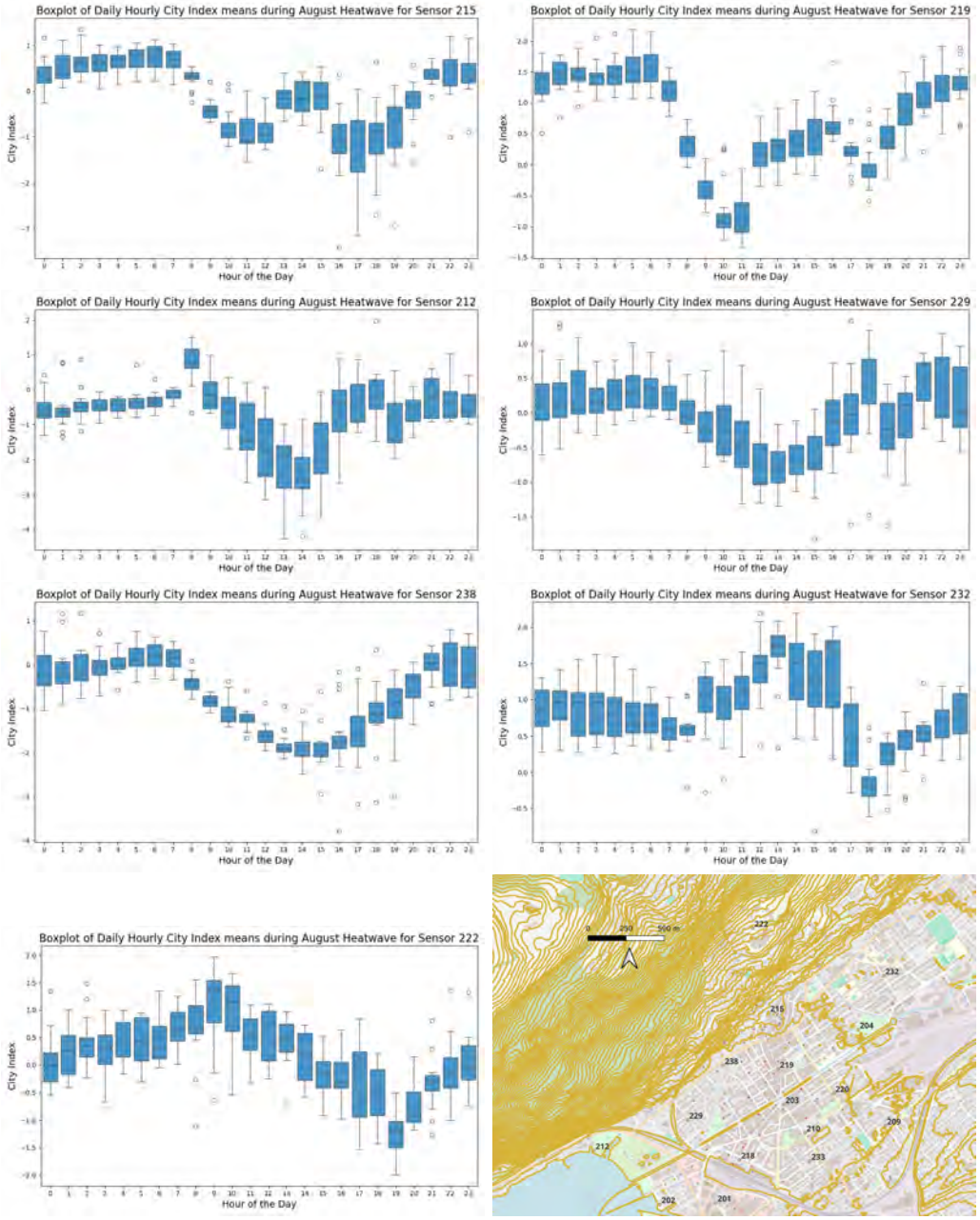

Figure 4.9: Hourly boxplots of mean City Index for the sensors located near the Northern edge of the central part of the city that may be susceptible to cold air infiltration during the early evening based on their position. Sensors 215, 238, 229, and 212 are located 150 meters or less from the base of the mountain. Sensor 219 and sensor 232 are about 350 meters away. Sensor 222 is located on the hill.

4.4 Fitnah

The results of Spearman's *Rho* and Kendall's *Tau* rank correlation tests and their p values shown in Figure 4.12 and 4.13 indicate that the FITNAH temperature layer is the best performing of the three FITNAH layers. It correlates significantly at p less than 0.05 with the empirical sensor data between 5 and 50 meters, loses five percent significance between 50 and 150 meters, and is again signficant beyond that. The UHI space and streets layers do not show significant correlations at buffers smaller than 100 meters, but as the buffer size increases, the p-value shrinks and both Spearman's *Rho* and Kendall's *Tau* increase. However, as the buffer size increases, all three FITNAH layers become both strongly and significantly correlated with the empirical data. For all three FITNAH output variables, the full summer 2023 results aligns closer than the heatwave 2023 dataset, although it is not clear that the difference is significant.

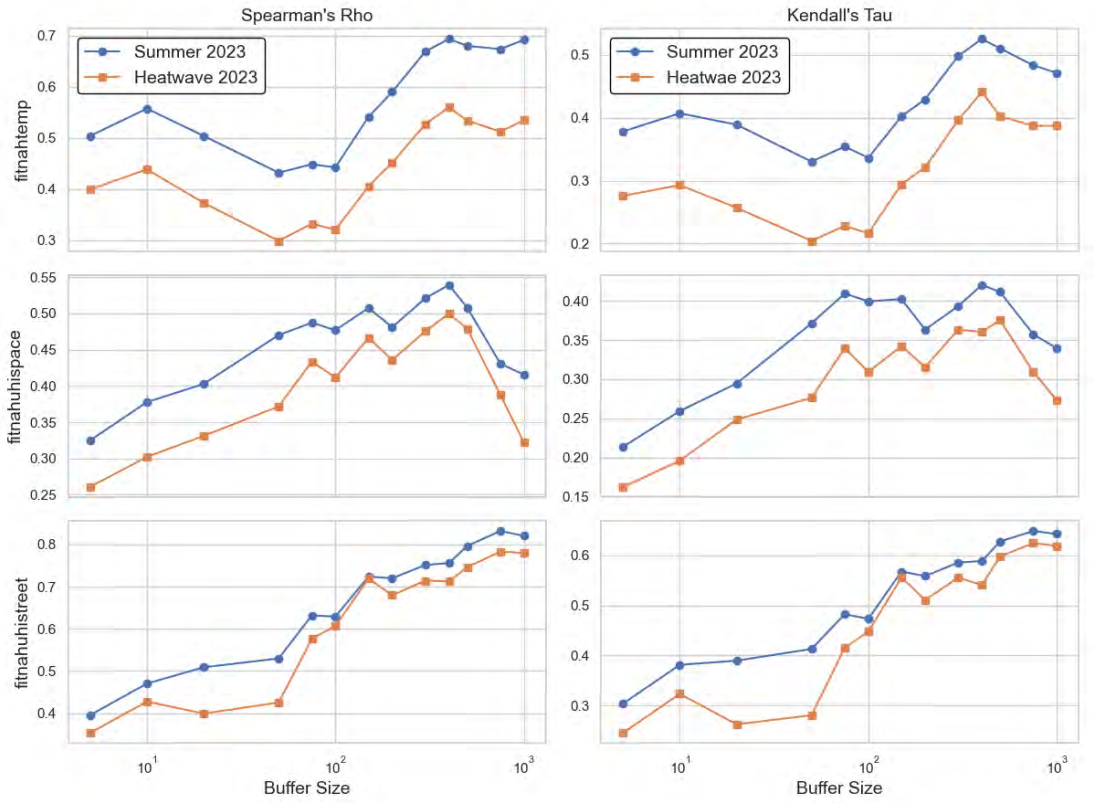

Figure 4.10: Results of the Spearman's *Rho* (left column) and Kendall's *Tau* (right column) ranking tests comparing the different FITNAH data layers to the empirical UHI at 4 AM during the heatwave and during the overall study period.

The correlation between the count of land use of types and the empirical UHI results depends on the indicator observed. Of the nine land-use types used in the FITNAH model inputs, five have enough values to produce rankings at lower buffers. These five with their respective p-values are plotted below. The *Building* and the *Paved* layers perform almost as well by these metrics as the Fitnah temperature layer and outperforms the UHI Streets and Spaces layers. Both *Building* and *Paved* are significant (or very close to it) at a five percent level across all buffers. The *Grass* category can also be effectively compared across relatively small buffer sizes and shows a signficant and strongly negative correlation with empirical UHI. The *Forest* category cannot be effectively

compared at lower buffers to the small amount of this land-use category within a small radius of an average city sensors, but it becomes strong significant and negatively correlated as the buffer size increases. On the other hand, *Water* is not significant at any buffer level, which is reflected in its move from slightly negatively to slightly positively correlated as buffer size increases.

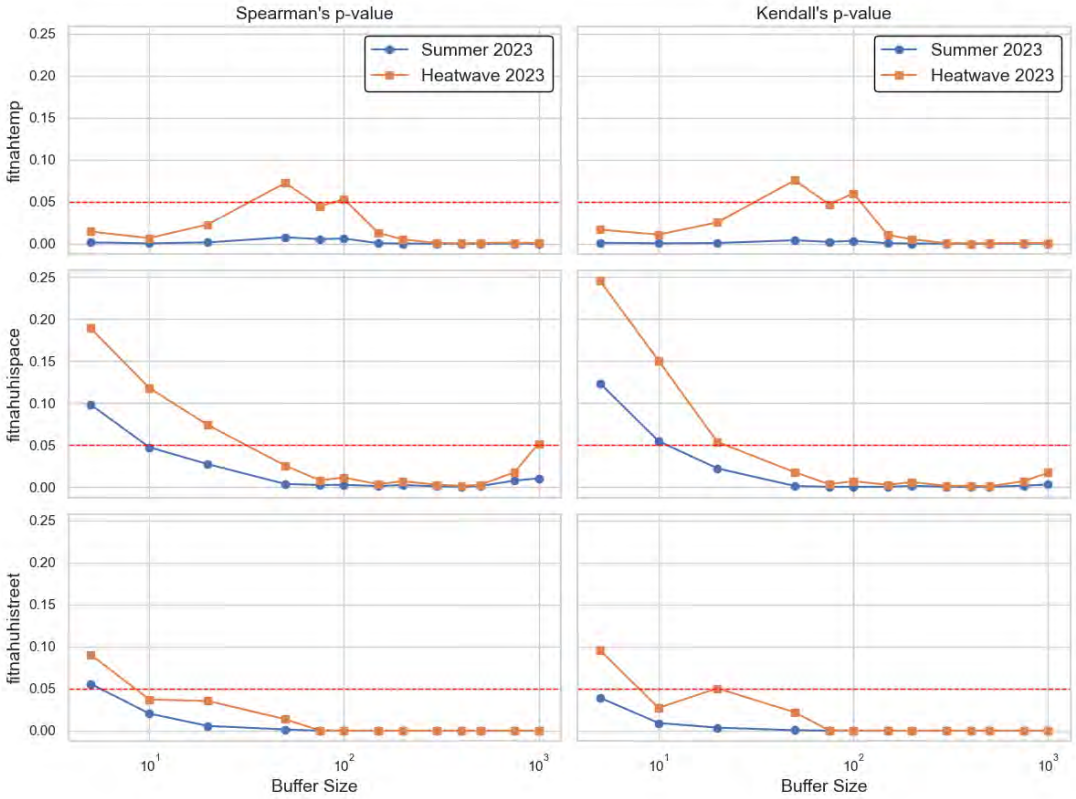

Figure 4.11: The p values from resulting from the Kendall's *Tau* and Spearman's *Rho* tests. The 0.05 signficance level is show in red.

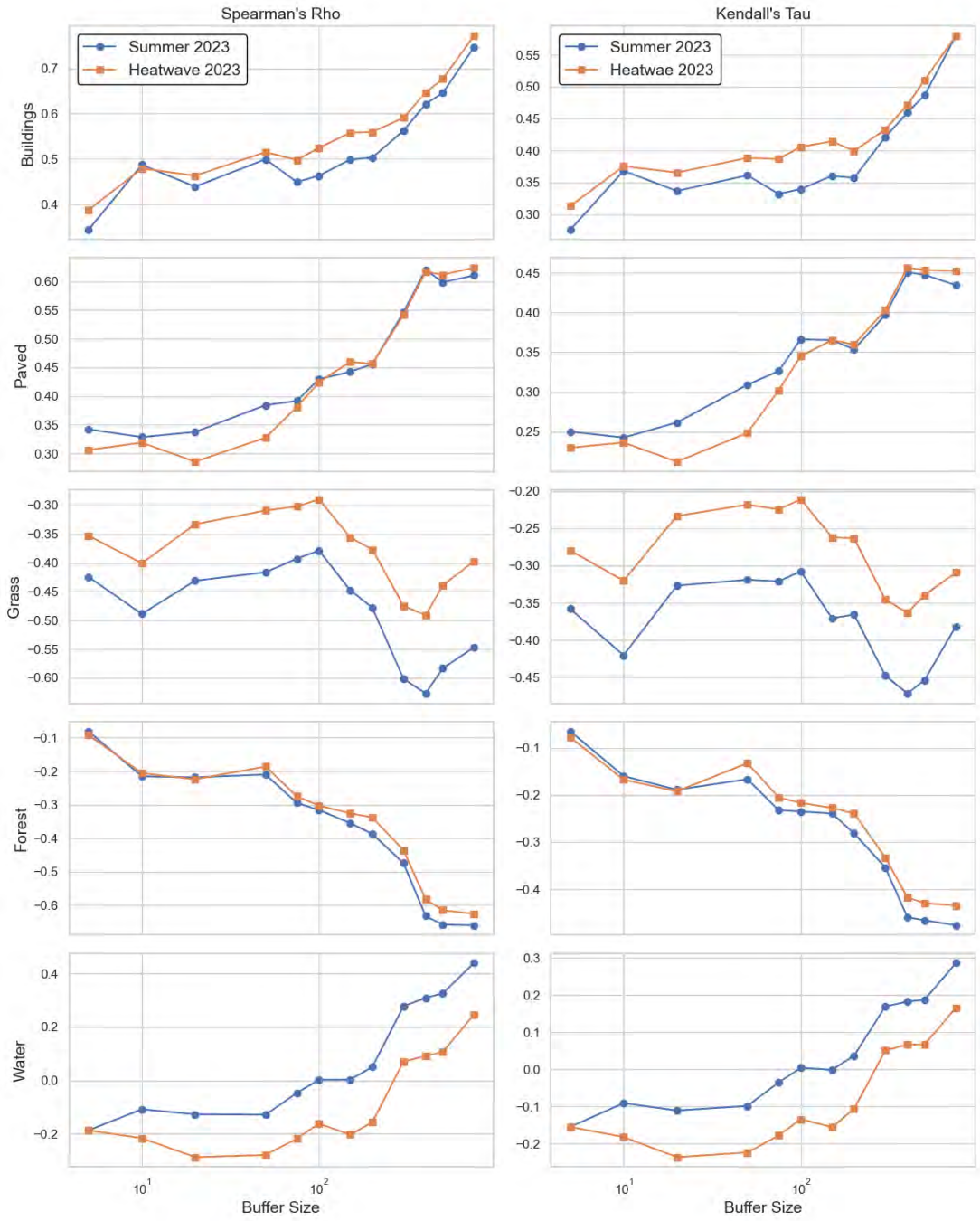

Figure 4.12: Results of the Spearman's *Rho* (left column) and Kendall's *Tau* (right column) ranking tests comparing the different landuse data categories used to calculate the FITNAH model to the empirical UHI at 4 AM during the heatwave and during the overall study period. Note the negative correlation of *Forest* and *Grass* and the positive correlations of *Paved* and *Buildings*

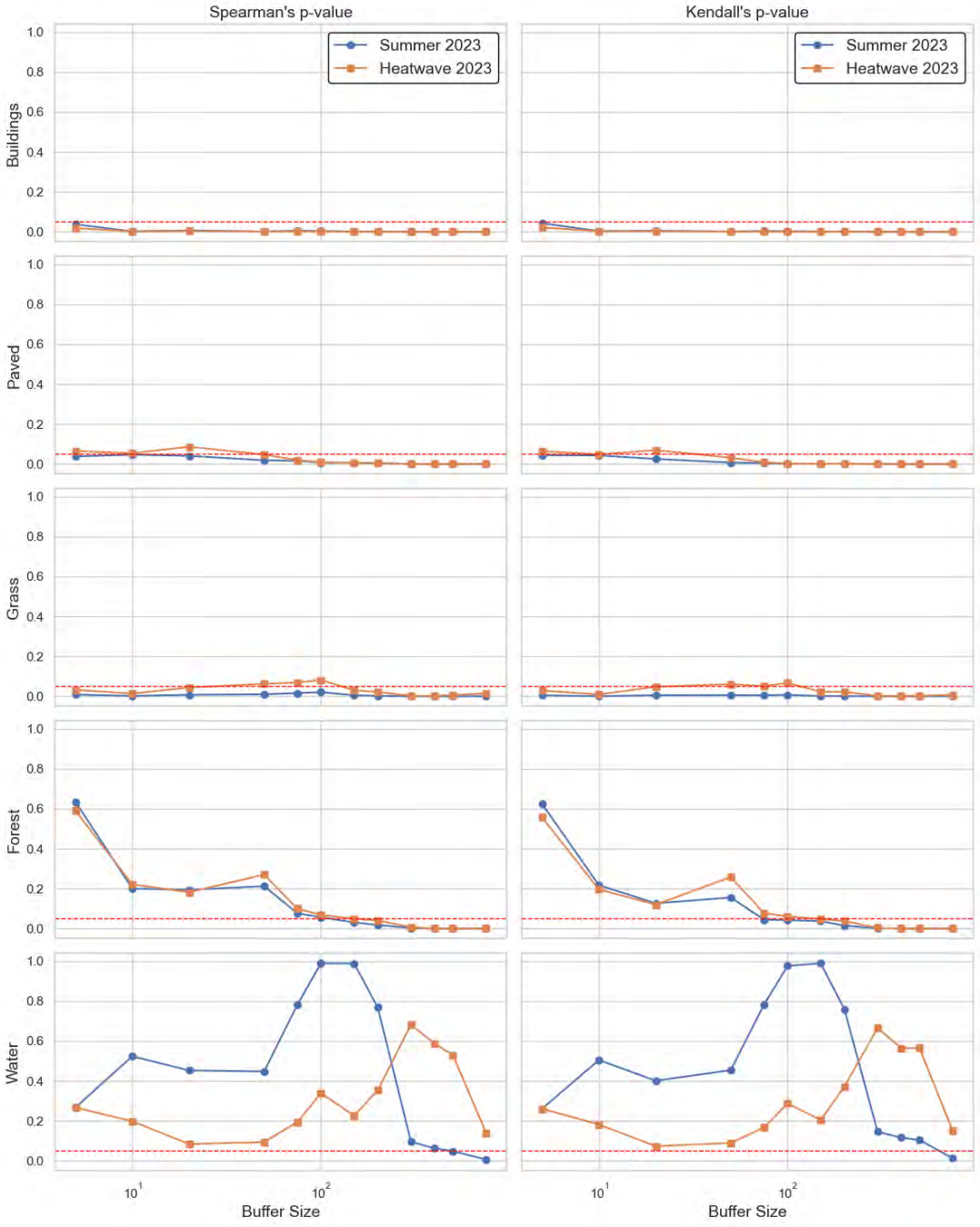

Figure 4.13: The p values from resulting from the Kendall's *Tau* and Spearman's *Rho* tests. The 0.05 signficance level is show in red.

Finally, the elevation and the slope of the sensors is also tested using Spearman's *Rho* and Kendall's *Tau*. Neither elevation nor slope are the results from the heatwave dataset reliably significant. The dataset from the full 2023 data is significant for elevation across buffer sizes. At the ten percent level, the mean elevation would be significant, while the slope would remain insignificant.

Bearing the significance tests in mind, the results show overall a negative correlation between altitude and UHI, which conforms to the hottest area of the ctiy being the low-lying central urban area (the Champagne and Central neighborhoods especially).

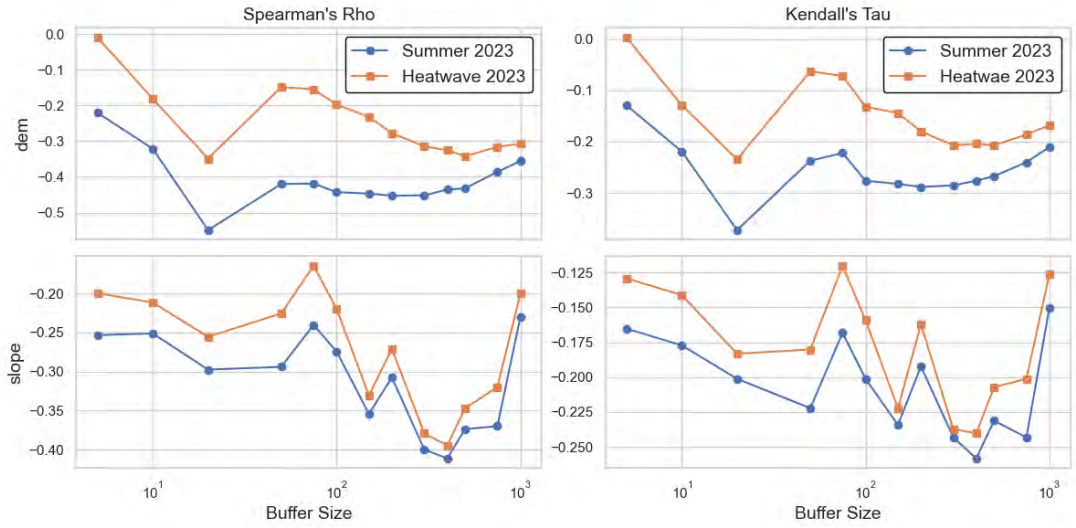

Figure 4.14: These plots show the results of the Spearman's *Rho* (left column) and Kendall's *Tau* (right column) ranking tests comparing the mean elevation and the mean slope to the empirical UHI at 4 AM during the heatwave and the overall study period.

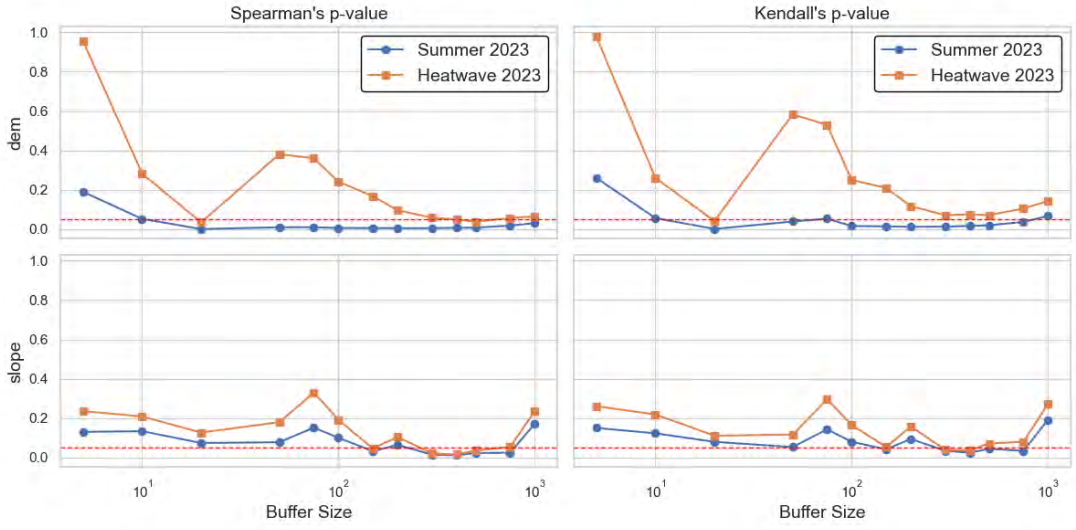

Figure 4.15: The p values from resulting from the Kendall's *Tau* and Spearman's *Rho* tests. The 0.05 signficance level is show in red.

The city index for all buffers less than 75 meters is calculated for all stations using the FITNAH data. This is subtracted from the empirical city index at 4AM on each day during the entire summer heatwave and the differences are presented in the following figures. Using this metric, the FITNAH

model overestimates the densest area of the city and the Bözingenfeld industrial zone, while it underestimates the rest of this city. This is evident in Champagne (205, 221), Mett (stations 205, 221, 228), Madretsch (233) and Mühlefeld(211) The strongest overestimation is in the Bözingenfeld industrial zone, and the strongest undersimtation is in the Champagne neighborhood. This distribution is the same when comparing the entire summer period and the heatwave period, as can be seen in both Figure 5.16 and 5.17

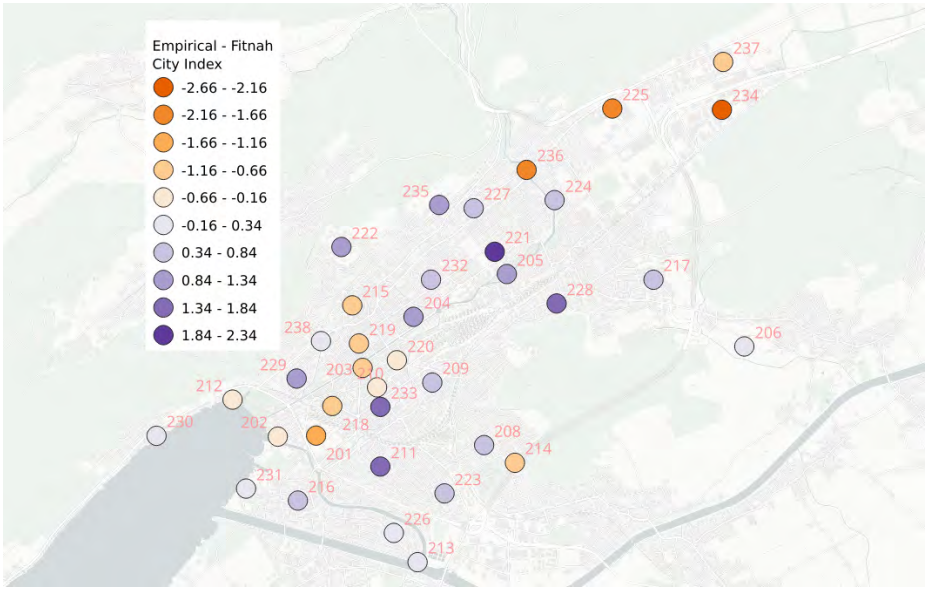

Figure 4.16: The difference between the city index of modeled and empirical data at each station over the entire summer 2023 period.

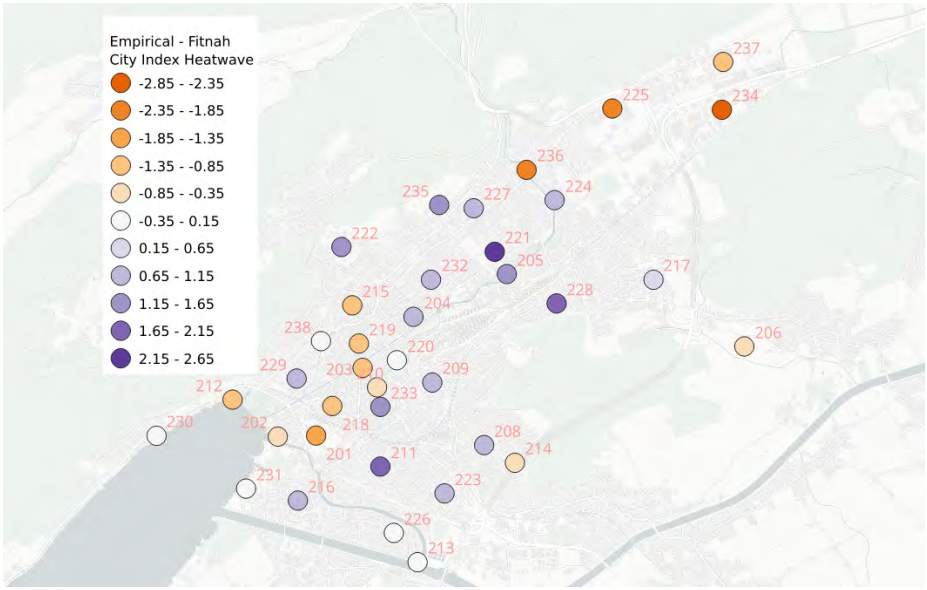

Figure 4.17: The difference between the city index of modeled and empirical data at each station oduring the summer 2023 heatwave.

Chapter 5

Discussion

Summer 2023 was a hot summer, with a strong heatwave. In general, the spatio-temporal distribution of the UHI, Tropical Nights and Summer days is consistent with past observations in Biel, the experience in Bern and common sense. Across all stations, the UHI displays the U-shaped diurnal evolution common in temperate, mid-latitude cities (Oke, 1982). The effect of previously identified local cold wind patterns and urban heat contours could be assessed. Comparing the ranking of empirical UHI to the station ranking of FITNAH and landuse data reveals that the FITNAH temperature, UHI and Space layers are marginally better correlated with the empirical data than some of the raw data inputs.

5.1 Bias

The temperature sensors have known biases due to the passive ventilation system that are especially impactful during the highest radiation periods of the day (Gubler et al., 2021 and Meyer et al., 2022). The difference between the SwissMetNet sensor and the Meteo reference LCD sensor was on the order of about 1.4°C during the day versus about 0.3°C at night, with a smaller bias available during the day. These results are in line with those reported since these sensors were first put into service in Bern in 2018 Gubler et al., 2021. This bias would mainly affect the two calculated measures of absolute temperature, the tropical nights and summer days, while the relative indicators (UHI and City Index) should remain unaffected.

This was accounted for by using a range of thresholds that demonstrate the number of summer days and tropical nights adjusting for different levels of bias. Figure 4.6 shows that the effect of changing the threshold for either summer days or tropical nights will certainly decrease the number of valid days in their respective categories, but there are not abrupt local changes due to these adjustments. For example, Station 203 would only gone down from 18 tropical nights to 17 tropical nights in the event of using a threshould for tropical nigths 0.5°C higher. This stability means the distributions of the tropical nights and summer days presented can be used with some confidence.

The second potential bias that was examined was the appropriateness of the rural reference sensor. The rural reference is located 1 kilometer from the city, 200 meters from the nearest neighborhood, 40 meters from the nearest farmhous, and is downwind of both the city and the Taubenlochwind. The reference itself, shown in figure 3.3, largely follows WMO guidelinesss (Organization, 2023). In addition, the temperatures at station 206 and 207 tend to match well throughout the day, thus indicating that station 206 is not unduly influenced by the city or local factors. There is a small decrease in station 206 relative to station 207 at 9 PM, but the drop in magnitude is slight and only lasts for one hour; this could be the influence of the cold air descending from the Jura. However, this flow of cold air is what would be happening if the city was not there, therefore the blockage of

this cold air flow is nonetheless a valid part of the UHI. Therefore, the rural reference chosen seems to be a good reference point for the conclusions drawn in the study.

The understanding of the potential bias can be improved using some of the methods used in Bern. The first is to install a second LCD meteo reference sensor at a height of two meters at the rural reference station (206) and the Swiss meteo reference station (207). The effect of radiative cooling can be more significant at two meters than at three meters, and in Bern this caused several "false" tropical night measurements in the three meter sensor [1]. This has been done at the SwissMeteo sensor but not at the rural reference sensor for the year 2024. The second method is to install more expensive, and therefore more reliable, sensors that are fully encased and self-ventilated preventing radiation bias and lack of ventilation bias. This method is also currently employed in Bern, with newer generation sensors overlapping with some LCD sensors, thereby providing information on the reliability of the urban LCD sensor network (Burger, Suter, et al., 2024).

5.2 Properties of Biel's UHI

The UHI values follow the same daily temporal pattern as consistently observed in studies in Bern; That is, an oscillation between a maximum around 04:00 and a minimum during the day (Gubler et al., 2021 and Meyer et al., 2022. Rain events significantly change the magnitude and temporal distribution of the UHI as shown by the June 30th rain event in Figure 5.2. The densest area of Biel, represented by sensors 203, 219 and 218 between the train station and the old city, recorded the highest UHIs over the whole period and during the August heatwave, reaching 3°C and 4°C respectively near 4 AM. On some days, the UHI reached 6°C at station 203 and 218, which is close to the highest values recorded in Bern. This is also in line with the highest UHI value recorded during the 1980s studies (Wanner, 1991). The lowest early-morning UHI values are on the periphery of the city and there is a more or less smooth transition from the hot zone of sensors 203, 219 and 218 into the background climate as can be seen in Figure 4.3

The effects of local factors such as local canyon geometry, topograhpy, presence of water and tree shading are visible throughout the data (Oke et al., 2017). The most prominent example of the effect of cold air flows is the Taubenloch Gorge sensor which recorded regular drops in temperature of 4 - 5 - 6 °C between 6 - 9 pm, This resulted in a seasonal mean UHI of almost -2°C at this time, about 4°C cooler than the city average. After this spike downwards, the Taubenloch gorge UHI gradually return to about 2°C by the early morning. Some of the other sensors at the base of the Beaumont mountain (219, 229, 232, 227, 212, 222) experienced relative temperature drops interrupting the general UHI pattern around this time, but none as clear-cut and obvious as at the Taubenloch Gorge sensor. Others (225, 215, 238) experienced no discernable change in trend during this period. Even for the sensors that do have a visible drop, the drop in cold air flow could be attributed to other factors such as local building geometry selectively shading the sensor.

The city index boxplots of Figures 4.7 - to 4.9 also illustrate the differential effects of shading on the evolution of the temperature differences in the city. Sensor 215 and sensor 209 (shown in figures 5.9 and 5.7 respectively) recieve sunlight only during the hours of approximately 12h00 - 14h00 leading them to experience a spike and subsequent drop in relative temperature. However, they are located in dense areas, so their relative temperature climbs back up as incoming solar radiation declines. The opposite effect can be seen with the Ile de la Suze sensor 205 in Figure 5.8. Due to a lack of shading the entire afternoon, this location is one of the hottest in the city at this time and experiences a local peak in its city index calculation during the hottest part of the day. Coming back to station 215, which is positioned to receive cold air flowing down the mountain, we can see that the simultaneous effect of canyon geometry and local cold air flows are difficult to disentangle during the daytime hours.

[1] This comes from discussion with Patrick Bigler and Moritz Gubler.

The lake front stations (202, 212, 230, 231, 239) all experienced negative UHI at noon. The coolest station throughout the day was located in the Nidau Forest (station 239), in a small woods some 150 meters from the lake. The second coolest lake front station is 231, which is also significantly shaded. While 212 and 230 are also lake front parks, the sensors are less underneath the tree canopy at station 231. The warmest lake front station is the 202 Biel Hafen station, which is surrounded by concrete and the water is filled with boats, unlike the other stations which are either grass (231, 212, 230) or gravel and leaves (239). Here, the UHI is barely negative at -0.26°C, which is comparable to city stations with a similar canyon geometry and surface material (203, 210, 201). The hottest areas at noon were located in the Champagne area (205, 221, 232) which is relatively dense, completely flat and blocked in from all sides by hills and urban development. At night, the lake front stations are not noticeably cooler than stations other than the main central warm area. Bözingenfeld is cooler at 4 AM than the lake front stations, which could be driven by the high heat capacity of water, which warms the surrounding air (Steeneveld et al., 2014).

The warmest daytime UHI values occurred in the Champagne neighborhood, in the Bözingenfeld industrial area and in the South of the city. Champagne and Bözingen are both relatively heavily built (LCZs 4,6 and LCZ 8 respectively) far from the lake, flat and blocked from the rest of the Plateau by the hills of the Längholz and Vorhölzli. It is therefore no surprise that these areas are hotspots during the day. Both central park stations, 204 and 205, recorded among the highest daytime temperatures, on par with the residential areas nearby. In time, it is likely that station 205 will also become much cooler during the day as the park is newly built and therefore the young trees are unable to provide significant shading during the afternoon. Station 204's heat is likely driven by its location outside of any shade during the afternoon period. Station 238, located in the city on a gravel path near one of the Suze canals and underneath shady trees, is the coolest non-lake and non-forest station during the day.

5.3 Comparison to the 1980s research

A quantitative comparison with the urban climate studies of the 1980s is not possible due to the different types of sensors used, the different placement of the sensors, and the different type of data collected. However, the resulting contour plots qualitatively compare quite well (see Figure 2.7 and 5.3). The heat contours taken during the hot summer day of 27.07.1983 lines up well with the heatwave results in this study for both the daytime (17:00 in 1983 vs 14:00 today) and for early evening (20:30 in 1983 vs 21:00 today). The results from the 15th - 16th July 1983 do not line up well with the heatwave results, but this is likely due to their occuring during an overcast day. Note the absolute temperature difference between the 9 PM measurement on the 15th of July and the 20h26 measurement on the 27th of July. Therefore, the early morning distribution on the 16th of July is difficult to compare with the distributions in the results. Two key things that are visible are the rapid decline in UHI in Bözingfeld and the peaks in the Champagne and central neighborhoods. The highest UHI reported in the earlier studies conforms with the UHI's observed during this study, around 6°C (Wanner, 1991).

5.4 Cold air infiltration

The cold air infiltration identified in the 1980s climate studies were investigated. While wind could infiltrate from many directions, the area focused on here was on the katabatic winds and the Taubenloch wind coming through the North of the city. The period chosen for a detailed comparison was the August heatwave period as that is when the UHI was at its peak and many of the associated phenomenon appear most visible in the data. The cooling effect as depicted in the box plots can be difficult to interpret. The onset of shade due to building configurations is clearly visible in some of the daytime differences that are clearly not attributable to these cold air effects. The comparison

between station 209 and station 203 between 10h00 and 15h00 shows the impact of direct sunlight versus the station being shaded. It is possible such patterns are influencing the results in the box plots presented for the cold air infiltration stations.

One certain wind effect, is the Taubenloch wind, shown in Figure 5.9. This is apparent in just about every single day of the summer period between the hours of 1800 and 2300. It is by far the strongest cooling wind effect visible in the dataset. The next station directly downwind and about 300 meters away, also shows a potential effect of the Taubenloch wind, but the signal strength has already decreased. The next stations potentially downwind, station 205, 217, 221, and 228 show sharp drops at 20h00 that may be attributable to the arrival of this cold air. As mentioned, this wind effect is not visible at the rural station, through the comparison with the swissmeteo station. Overall, the taubenlochwind is clearly visible at the mouth of the gorge and the effect can be seen in downstream stations, with a much less significant effect.

The effect of the katabatic winds was identified to be much smaller than the Taubenlochwind (Wanner, 1991). At the stations near the Taubenloch, both 227 and 235 show a relative cooling that begins in the afternoon and ends around 20h00. Station 225 shows a stabilization of temperatures around 20h00 and only exhibits cooling later in the night. Station 225 is located on a wide street about 40 meters from the base of the mountain with no obstructions and would therefore be expected to see the wind effect. To the west of the Taubenloch gorge, Station 227 shows a relative cooling compared to the rest of the city over the afternoon which may be attributable to its position on the incline of the hill facing South or due to the cooler air flowing down from above.

The city center stations at the base of Beaumont showed similar results in Figure 4.10. The sensor at the highest elevation, Beaumont 222, shows a large drop in relative temperature at 19h00. Two of the three stations that most directly abut the mountain show no clear effect (old city 215 and museum 238). Station 212, on the lake and the mountain, shows about a 0.5°C drop in relative temperature between 19h00 and 20h00. The stations about 300 meters from the base of the mountain, (city center 219, viaduct 229 and champagne 232) do appear to show drops in temperature at the critical 19h00 - 20h00 period, but it is not clear where this air is coming from as it is not clearly visible in the stations that abut the mountain face.

In general the resuls show a strong Taubenloch wind effect between 18h00 and 21h00 near the mouth of the gorge that diminishes with distance as the air spreads across the city. The katabatic winds are difficult to discern using these boxplot methods since they are smaller in magnitude and may be caused by other factors such as building geometry. Nonetheless, cold air flow is clearly visible in the two stations on the mountain face (222 and 235). This analysis could be improved by taking windspeed measurements or by expanding the sensor network to include additional sensors around the Taubenloch wind area.

5.5 Tropical Nights and Summer Days

The distribution of tropical nights and summer days follows the distribution of the UHI values in the evening and the day, respectively. The tropical nights occurred almost exclusively during the heatwave periods, even at relatively warm stations in the center of the city. The number of excess summer days shows divergent patterns based on the characteristics of the station. The cool stations around the lake accumulated a significant number of negative summer days; Nidau Forest (239) recorded 29 fewer summer days than the rural station. Station 204 recorded the highest number of excess summer days with 13, followed by the Champagne Blumen with 12. At the same time, the high number of tropical nights recorded in the center of the city, between 18-19, at stations 203, 218 and 220 is cause for concern, compared to zero tropical nights being recorded at the rural reference station. This is robust to increasing the tropical night threshold by 0.5 or 1°C - of course the number of nights will fall but remains elevated at 17, for station 218 at the train station. As reviewed in the introduction this can have serious health impacts over the long term and during the acute periods

of heat (M. S. Ragettli et al., 2017 and M. Ragettli et al., 2020).

In addition, the extra heat during the day at the central parks of 204 and 205, as well as the broad hotspot throughout the Champagne neighborhood is notable. The extra heat in this region may influence the development and political environment locally, as it may add pressure for activist groups to fight to maintain access to cool and green spaces in this urban hotspot. A second important factor pointed out by the relative heat of 205 is the long timeframe it can take for urban heat mitigation factors to take effect. The trees planted during the recent renovation of the Ile de la Suze are relatively young and do not yet provide signficant shade relief in the green area itself. This will change with time, but highlights the need to plan ahead when implementing urban heat mitigation strategies.

One location that stands out is the museum sensor 238. It has a very low number of summer days and tropical nights, and it features all of the elements that are frequently discussed in urban heat mitigation literature. It is located next to a branch of the Suze, under well-developped shady trees and the ground is a permeable mix of grass and dirt and gravel. Despite being located in an otherwise warm area of the city, it had 15 fewer summer days than the rural reference station, the largest for any sensor that has a full set of data for the summer period. At the same time, there are 8 troopical nights, which is more than the Bözingefeld sensors (3-6) and comparable to sensors in the middle of the urban agglomeration. It is probably not possible to provide more mitigation that that arleady in place station 238, which is reflected by the low excess summer days value, but the tropical nights remain relatively high.

5.6 Ranking Tests

The results of the Kendall's tau and Spearman's rho ranking tests comparing the FITNAH data to empirical results point to a few interesting lines of discussion. Broadly, the KT and SR tests have the same patterns and similar magnitudes. KT is lower nearly across the board for the FITNAH layers. The full FITNAH temperature layer tends to correlate more closely with the empirical data than with the separate UHI Space and UHI Street layers, in particular at buffers below 100 meters. For all FITNAH layers, the correlation and signficance increases with buffer size. The reason this happens at lower buffers is likely due to issues of representativity and missing data. When a mean is taken of all the data intersecting the buffered circle, a larger circle implies a more representative average of the local model outputs, at the cost of losing accuracy. Considering the FITNAH temperature layer at five meters, only about 4 model output squares are used in the mean. Considering the UHI layers, even fewer values will be available and many lower buffers located not directly on a street will be empty; this leads to very high p values and meaningless ranking coefficients at small buffer values. Of the three FITNAH layers, only the Temperature layer has significant results at low buffer layers. However, by about a 100 meter buffer radii, even the UHI space and street layers have enough values to take a representative mean and have enough data across all sensors for interpretable rankings. By this time however, they no longer represent the microscale measurement of the 10m FITNAH data and are more representative of the LCZ scale.

At a buffer radii of 500 - 1000 meters the discrimination between sensors is made on whether it is in the middle of the city or closer to the edge of the city rather than on the local characteristics of the sensor location. Both the KT and SR correlation coefficients rise significantly from about 100 meters onward. This is backed up by the pattern of the temperature layer: there is a SR coefficient of about 0.5 at 5-10 meters, a decline at buffers of 20 and 50 meters and improvement again from 75 meter buffer radii onward. This suggests the raw model output, the temperature layer, performs well enough at low buffer sizes and suggests that if the UHI layers had more data in them, they would also correlate more closely with the empirical results. The effectiveness of using an indicator that accounts for the location's relative position in the city in predicting the UHI speaks to the importance of the macro effects driving UHI mentioned in the introduction, namely the amount of

concrete buildings emitting and blocking radiation (Oke, 1982).

Looking at the landuse data, the landuse types Paved, Grass and Buildings are all significant and strongly correlated with the empirical data. Like with the FITNAH Temperature layer, the correlation coefficients increase with buffer size, and the heatwave results are less well correlated than the overall results. Water and Forest, and the rest of the variables not shown, are not signficant or meaningful largely due to the lack of data available for the landuse type used in the analysis. A subgroup analysis comparing stations around the lakefront or near the edge of the city could be a way to analyze these values. The elevation and slop values are less strongly correlated with the empirical results than the FITNAH layers or the land use values, but only elevation is signficantly correlated using the summer 2023 dataset.

The effectiveness of using the count of buildings or paved areas compared to the FITNAH temperature, UHI and Space layers is an interesting result. It suggests that the FITNAH model is not a signficant improvement over simply using a spatial mean of existing land-use data available to all city planners in Switzerland. It also suggests that using a landuse regression technique that takes advantage of the known relationship between these key variables (and others) could provide a more effective prediction of the UHI. In Bern, such a statistical model has been developed and tested and has shown to be more closely correlated to the empirical results than the Bern FITNAH data (Burger et al., 2022). In this case, the comparison was done with a detailed FITNAH dataset created specifically for the city of Bern and a model trained on years of data collected from Bern. Neither of these are therefore directly comparable to the situation in Biel, where a model would be trained and tested on less data and the FITNAH data is a lower resolution cantonal model. However, the evidence suggests that even a relatively simple linear model could perhaps be as fruitful for predicting the regions with the highest UHI as the FITNAH model.

The correlations are robust to other subsets of the data, such as using the 5 AM, 4-6 AM, UHI and City Indexes instead of ranking the 4 AM UHI which is presented in the results section. It is also robust to using individual periods, such as all of July 2023 and all of August 2023, which implies that the relationship can be trusted. The analysis was also repeated with the forest sensors and sensors with missing data removed. Again, the results were exactly comparable.

5.7 Geographic limitations

The network does a satisfactory job covering the commune of Biel and the closest areas of Nidau. In general, additional sensors could be useful due to the topography of the city and the diversity of the built environment. There are some neighborhoods of Biel/Bienne which do not have good sensor coverage, such as *Mett*, and the *Linde Quartier* which lies between logger 209 and the *Langholz*. One important LCZ that is missing from the coverage is the main industrial zone in the center of the city that comprises a large CFF logistics depot and adjoining (often repurposed e.g. for rockclimbing and skateboarding parks) industrial facilities. Either side of the zone is covered, however the zone itself is not, which may complicate interpretation of the UHI distribution in this critical sector.The hillside neighborhoods above the old city, and below the 222 Hospital sensor, also do not have much sensor coverage.

Beyond the city itself, there is continuous urban terrain between Biel, Port, Nidau and Brügg as can be seen from the OpenStreetMaps presented previously. While stations 231, 239 and 216 were located in Nidau and stations 228 and 213 are in Port, the transition from urban to rural cannot be observed in the South / South Western direction due to the additional urbanized area that lays beyond the boundaries of Biel. Looking North, the communes of Evilard and Macolin are not observed, although sensor(s) were included in the 2024 dataset. Difficulties in arranging permissions to access the Längholz hampered the position of the forest sensor leading to its placement on the edge of the forest. Further it is on a sharp incline, in a section of a 'clear forest' that has recently experienced signficant thinning and changes in anticipation of its conversion into a forest cemetery.

Its representativity of the forest therefore is unlikely.

Chapter 6

Conclusion

This master dissertation set up an in-situ temperature sensor network to measure the spatial and temporal variation of the UHI across Biel and compare the results to a recent modeling exercise commissioned by the canton of Bern. It reaches a maximum in the early morning in the center of the city at around 4 AM (6°C on some days) and a minimum during the daytime in a section of woods near the lake. The distribution of tropical nights and summer days closely follows the distribution of the UHI in the early morning and in the early afternoon, respectively. The study coincided with a severe heatwave during August 2023 and the results show the impact of the UHI on heat indicators: nearly 20 tropical nights were recorded in the urban center compared to 0 at the rural reference location.

A deeper dive is needed to explore the dynamics of the nocturnal air flows that can bring relief to the UHI. While the Taubenlochwind is clearly visible using the boxplots provided, the smaller winds are not so obvious and the station variability can mask these effects. A more rigorous statistical approach could isolate them, in particular if additional stations were set up explicitly for this task. The results of comparing the FITNAH model data and land use data suggest that using the simple relationships between buildings or paved areas and the UHI already performs as well as the FITNAH model in terms of predicting the location of hot spots for small-medium sized cites. This suggests as well that a land-use regression model could be a productive and low cost alternative to a physical model.

As the new set of climate models is set to be released in 2025 for Switzerland, it would be an enormous benefit to use the climate data and look at how temperature may evolve in Biel. Whether this involves dynamic changes in land use, or simply applying a land use regression model using existing data, it will be critical to take into account the effect of the UHI when looking at the impact of increased temperatures and heatwaves on thermal comfort using these datasets.

Bibliography

Arndt, S., Turvey, C., & Andreasen, N. C. (1999). Correlating and predicting psychiatric symptom ratings: Spearman's r versus kendall's tau correlation. *Journal of psychiatric research*, *33*(2), 97–104. https://doi.org/10.1016/s0022-3956(98)90046-2

Berkeley Earth. (2024). Global temperature report for 2023 [Accessed: 2024-09-15]. https://berkeleyearth.org/global-temperature-report-for-2023/

Berlincourt, P. (1988). *Les émission atmosphériques de l'agglomération de bienne* (PhD Thesis). Universität Bern.

Brönnimann, S. (2018). *Klimatologie*. Haupt Verlag.

Bundesamt für Umwelt (BAFU). (2018). Hitze in städten: Grundlage für eine klimaangepasste siedlungsentwicklung.

Bundesamt für Umwelt BAFU. (2024a). Hydrologiesche daten und vorhersagen [Aare - Brügg, Aegerten, Accessed: 2024-04-17]. https://www.hydrodaten.admin.ch/de/seen-und-fluesse/stationen-und-daten/2029#temperature-annual

Bundesamt für Umwelt BAFU. (2024b). Hydrologiesche daten und vorhersagen [Accessed: 2024-04-17]. https://www.hydrodaten.admin.ch/de/seen-und-fluesse/stationen-und-daten/2307#temperature-annual

Burger, M., Suter, I., Anet, J., Gubler, M., Tinner, N., & Brönnimann, S. (2024). Erfassung von stadtklima-massnahmen – methodische erkenntnisse aus bern und zurich. *Geographica Bernensia*, *G106*. https://doi.org/10.4480/GB2024.G106

Burger, M., Gubler, M., & Brönnimann, S. (2022). Modeling the intra-urban nocturnal summertime air temperature fields at a daily basis in a city with complex topography. *PLOS Climate*, *1*(12), 1–20. https://doi.org/10.1371/journal.pclm.0000089

Burger, M., Gubler, M., Holtmann, A., & Brönnimann, S. (2024). Spoilt for choice - intercomparison of four different urban climate models. *Urban Climate*, *58*, 102166. https://doi.org/https://doi.org/10.1016/j.uclim.2024.102166

Casanueva, A., Kotlarski, S., Liniger, M., Schwierz, C., & Fischer, A. (2023). Climate change scenarios in use: Heat stress in switzerland. *Climate Services*, *30*, 100372. https://doi.org/https://doi.org/10.1016/j.cliser.2023.100372

Demuzere, M., Kittner, J., & Bechtel, B. (2021). Lcz generator: A web application to create local climate zone maps. *Frontiers in Environmental Science*, *9*, 637455. https://doi.org/10.3389/fenvs.2021.637455

de Schrijver, E., Bundo, M., Ragettli, M. S., Sera, F., Gasparrini, A., Franco, O. H., & Vicedo-Cabrera, A. M. (2022). Nationwide analysis of the heat- and cold-related mortality trends in switzerland between 1969 and 2017: The role of population aging. *Environmental Health Perspectives*, *130*(3), 037001. https://doi.org/10.1289/EHP9835

Dubler, A., & Martin, P. (2018). Biel (be, gemeinde).

Ein neues stück stadt [Accessed: 2024-06-05]. (n.d.).

Elmarakby, E., & Elkadi, H. (2024). Impact of urban morphology on urban heat island in manchester's transit-oriented development. *Journal of Cleaner Production*, *434*, 140009. https://doi.org/https://doi.org/10.1016/j.jclepro.2023.140009

Elmqvist, T., Fragkias, M., Goodness, J., Güneralp, B., Marcotullio, P. J., McDonald, R. I., Parnell, S., Schewenius, M., Sendstad, M., Seto, K. C., & Wilkinson, C. (2013). *Urbanization, biodiversity and ecosystem services: Challenges and opportunities: A global assessment*. Springer. https://doi.org/10.1007/978-94-007-7088-1

Fan, C., & Wang, Z. (2020). Spatiotemporal characterization of land cover impacts on urban warming: A spatial autocorrelation approach. *Remote Sensing*, *12*(10). https://doi.org/10.3390/rs12101631

Geonet. (2022). Erstellung einer klimaanalyse und planungshinweiskarte klima für den kanton luzern.

Geonet. (2023a). Erstellung einer klimaanalyse und planungshinweiskarte für den kanton luzern.

Geonet. (2023b). Klimaökologische situation im kanton bern: Modellbasierte klimaanalyse.

Geonet. (2024a). Analyse climatique du canton de neuchâtel.

Geonet. (2024b). Analyse der klimaökologischen funktionen und prozesse für das gebiet des kantons aargau.

Grize, L., Huss, A., Thommen, O., Schindler, C., & Braun-Fahrländer, C. (2005). Heat wave 2003 and mortality in switzerland. *Swiss Medicine Weekly*. https://doi.org/10.4414/smw.2005.11009

Gubler, M., Christen, A., Remund, J., & Brönnimann, S. (2021). Evaluation and application of a low-cost measurement network to study intra-urban temperature differences during summer 2018 in bern, switzerland. *Urban Climate*, *37*. https://doi.org/https://doi.org/10.1016/j.uclim.2021.100817

Hadorn, W. (2012). *Hans stockli, ou 20 ans d'essor de la ville de bienne*. Bureau Cortesi Bienne.

Huang, W. T. K., Masselot, P., Bou-Zeid, E., Fatichi, S., Paschalis, A., Sun, T., Gasparrini, A., & Manoli, G. (2023). Economic valuation of temperature-related mortality attributed to urban heat islands in european cities. *Nature Communications*.

IPCC. (2023). *Summary for policymakers. in: Climate change 2023: Synthesis report. contribution of working groups i, ii and iii to the sixth assessment report of the intergovernmental panel on climate change* (C. W. Team, H. Lee, & R. J, Eds.). https://doi.org/10.59327/IPCC/AR6-9789291691647.001

Kottek, M., Grieser, J., Beck, C., Rudolf, B., & Rubel, F. (2006). World map of the köppen-geiger climate classification updated. *Meteorologische Zeitschrift*, 259–263.

Kuttler, W. (2008). The urban climate – basic and applied aspects. In J. M. Marzluff, E. Shulenberger, W. Endlicher, M. Alberti, G. Bradley, C. Ryan, U. Simon, & C. ZumBrunnen (Eds.), *Urban ecology: An international perspective on the interaction between humans and nature* (pp. 233–248). Springer US. https://doi.org/10.1007/978-0-387-73412-5_13

Laboratoire cantonal de la protection des eaux et du sol. (2023). Rapport sur l'état des eaux 2019-2023.

Martin-Vide, J., Sarricolea, P., & Moreno-García, M. C. (2015). On the definition of urban heat island intensity: The "rural" reference. *Frontiers in Earth Science*, *3*. https://doi.org/10.3389/feart.2015.00024

MeteoSwiss. (2018). Ch2018 – climate scenarios for switzerland.

MeteoSwiss. (n.d.). Climate indices [Accessed: 2024-06-03]. %5Curl%7Bhttps://www.meteoswiss.admin.ch/services-and-publications/applications/ext/climate-indicators-public.html%7D

Meyer, L., Gubler, M., Meier, F., & Brönnimann, S. (2022). Intercomparison and combination of low-cost urban air temperature measurement approaches. *Meteorologische Zeitschrift*, *31*(2), 131–148. https://doi.org/10.1127/metz/2021/1107

Morisson, A., & Gong, H. (2024). Leveraging national opportunities for regional transformation: Multi-scalar system-building and legitimation in a swiss industrial town. *European Planning Studies*, *32*(3), 607–628. https://doi.org/10.1080/09654313.2023.2247023

Oke, T. R. (1981). Canyon geometry and the nocturnal urban heat island: Comparison of scale model and field observations. *Journal of Climatology*, *1*(3), 237–254. https://doi.org/https://doi.org/10.1002/joc.3370010304

Oke, T. R. (1982). The energetic basis of the urban heat island. *Quarterly Journal of the Royal Meteorological Society*, *108*(455), 1–24. https://doi.org/https://doi.org/10.1002/qj.49710845502

Oke, T. R., Mills, G., Christen, A., & Voogt, J. A. (2017). *Urban climates*. Cambridge University Press.

Organization, W. M. (2023). Guidance on measuring, modelling and monitoring the canopy layer urban heat island (cl-uhi). *World Meteorological Organization*.

Puka, L. (2011). Kendall's tau. In *International encyclopedia of statistical science* (pp. 713–715). Springer. https://doi.org/10.1007/978-3-642-04898-2_324

Ragettli, M., Röösli, M., & Walter, E. (2020). *Gesundheitliche auswirkungen von hitze in der schweiz und die bedeutung von präventionsmassnahmen: Hitzebedingte todesfälle im hitzesommer 2019 – und ein vergleich mit den hitzesommer 2003, 2015 und 2018*. Swiss Tropical; Public Health Institute.

Ragettli, M. S., Vicedo-Cabrera, A. M., Schindler, C., & Röösli, M. (2017). Exploring the association between heat and mortality in switzerland between 1995 and 2013. *Environmental Research*, *158*, 703–709. https://doi.org/https://doi.org/10.1016/j.envres.2017.07.021

Rickli, R. (1988). *Untersuchungen zum ausbreitungsklima der region biel* (PhD Thesis). Geographisches Institut der Universität Bern.

Rickli, R., & Wanner, H. (2019). Feldexperiment im raum biel - datenkatalog.

Rinner, C., & Hussain, M. (2011). Toronto's urban heat island—exploring the relationship between land use and surface temperature. *Remote Sensing*, *3*(6), 1251–1265. https://doi.org/10.3390/rs3061251

RJB. (2023). L'initiative biennoise "climat urbain" a abouti [Accessed: 2024-09-15]. https://www.rjb.ch/rjb/Actualite/Region/20230224-L-initiative-biennoise-Climat-urbain-a-abouti.html

Robine, J.-M., Cheung, S. L. K., Roy, S. L., Oyen, H. V., Griffiths, C., Michel, J.-P., & Herrmann, F. R. (2008). Death toll exceeded 70,000 in Europe during the summer of 2003. *Comptes Rendus. Biologies*, *331*(2), 171–178. https://doi.org/10.1016/j.crvi.2007.12.001

Schüssinsel [Accessed: 2024-06-05]. (n.d.).

Stadt Bern. (2024). Hitzebelastung in der stadt bern [Accessed: 2024-05-30].

Stadt Zürich. (2024). Hitze [Accessed: 2024-05-30].

Steeneveld, G., Koopmans, S., Heusinkveld, B., & Theeuwes, N. (2014). Refreshing the role of open water surfaces on mitigating the maximum urban heat island effect. *Landscape and Urban Planning*, *121*, 92–96. https://doi.org/https://doi.org/10.1016/j.landurbplan.2013.09.001

Stewart, I. D., & Oke, T. R. (2012). Local climate zones for urban temperature studies. *Bulletin of the American Meteorological Society*, *93*(12), 1879–1900. https://doi.org/10.1175/BAMS-D-11-00019.1

Swiss Federal Statistical Office (BFS). (2024a). Räumliche gliederungen [Accessed: 2024-05-30]. https://www.bfs.admin.ch/bfs/de/home/statistiken/regionalstatistik/kartengrundlagen/raeumliche-gliederungen.assetdetail.30665938.html

Swiss Federal Statistical Office (BFS). (2024b). Structure of the permanent resident population by canton, 2010-2023 [[Accessed: 2024-12-07]"].

Système d'Information du Territoire à Genève (SITG). (2024). Fiche de métadonnée: Analyse climatique 2020 - ilot de chaleur nocturne 2020-2049 [Accessed: 2024-11-15].

Terrain gurzelen home [Accessed: 2024-06-05]. (n.d.).

Vicedo-Cabrera, A. M., de Schrijver, E., Schumacher, D. L., Ragettli, M. S., Fischer, E. M., & Seneviratne, S. I. (2023). The footprint of human-induced climate change on heat-related deaths in the summer of 2022 in switzerland. *Environmental Research Letters*, *18*(7). https://doi.org/10.1088/1748-9326/ace0d0

Ville de Genève. (2024). Stratégie climat: Aménagement du territoire [Accessed: 2024-05-30].

Virtanen, P., Gommers, R., Oliphant, T. E., Haberland, M., Reddy, T., Cournapeau, D., Burovski, E., Peterson, P., Weckesser, W., Bright, J., van der Walt, S. J., Brett, M., Wilson, J.,

Millman, K. J., Mayorov, N., Nelson, A. R. J., Jones, E., Kern, R., Larson, E., ... SciPy 1.0 Contributors. (2020). SciPy 1.0: Fundamental Algorithms for Scientific Computing in Python. *Nature Methods*, *17*, 261–272. https://doi.org/10.1038/s41592-019-0686-2

Wanner, H. (1991). *Bienne: Climat et pollution atmosphérique dans une ville suisse*. Haupt Verlag. https://boris.unibe.ch/185035/

Wellinger, N., Gubler, M., Müller, F., & Brönnimann, S. (2024). Gis-based revision of a wudapt local climate zones map of bern, switzerland. *City and Environment Interactions*, *21*, 100135. https://doi.org/https://doi.org/10.1016/j.cacint.2023.100135

West Ast. (2024). West ast [Accessed: 2024-09-15]. https://westast.ch/wordpress/

Chapter 7

Annex 1

7.1 Software and Algorithsm used for the data analysis

Software and Tools Used
Software: Pycharm for coding, TexStudio for LaTeX editing, and QGIS for geospatial analysis and map creation.
Python Packages: *scipy* for statistical tests (Kendall's Tau and Spearman's Rho), *xarray* and *pandas* for data management and preparation, *geopandas* and *rasterio* for handling geospatial data.
Plots and Visualizations: All plots were generated using *matplotlib*.
Maps: All maps were created using QGIS.
AI Assistance: ChatGPT, PyCharm AI Assistant, and GitHub Copilot were used solely for formatting and programming purposes.

Table 7.1: Summary of Software, Python Packages, and Tools Used

7.2 Summary Table of Sensors

X Coordinate	Y Coordinate	Name	Group	Neighborhood	Sensor ID
2585014.11086987	1219998.17016653	Robert-Walser-Platz	Hot	Bahnhof	201
2584647.01086331	1219988.27016833	Hafen	Water	Lake	202
2585459.51087453	1220646.07017044	Zentralplatz	Hot	Center	203
2585946.81088076	1221134.77017259	Stadtpark	Green	Center	204
2586841.31089471	1221544.27017185	Ile de la Suze	Green	Champagne	205
2589116.21093916	1220851.17015334	Rural reference	Reference	None	206
2598212.21107792	1225339.17014795	Swiss Meteo Reference	Reference	None	207
2586623.50163489	1219907.00302359	Möösli	Suburb	Möösli	208
2586127.00435491	1220505.75806624	Madretsch-Piano	Residential	Madretsch	209
2585597.90543899	1220459.86008397	Congresshaus	Hot	Center	210
2585629.30380887	1219701.80705616	Mühlefeld	Suburb	Mühlefeld	211
2584213.40868293	1220342.51613918	Seepark	Water	Lake	212
2585986.20708087	1218786.66309739	Port NBK	Water	Port	213
2586918.50109055	1219738.00201541	Längholz	Forest	None	214
2585360.40543482	1221244.56008834	Old City	Center	Old City	215
2584839.50652196	1219376.51209687	Nidau-Mittestrasse	Residential	Nidau	216
2588246.30546011	1221489.56008199	Geyisreid	Residential	Mett	217
2585169.01087119	1220281.52016844	Bahnhof	Center	Bahnhof	218
2585424.00489271	1220879.50907778	New City	Center	Center	219
2585787.80489602	1220719.45907625	Altersheim-Neumarkt	Health	Center	220
2586725.30544576	1221757.26008724	Champagne-Piano	Residential	Champagne	221
2585256.50543244	1221802.96009127	Spital	Health	Beaumont	222
2586244.5087159	1219444.71612385	Altersheim-Erlacher	Health	Mühlefeld	223
2587298.75490466	1222251.3840793	Bözingen	Taubenloch	Bözingenfeld	224
2587851.8054523	1223128.01009083	Swisstennis	Industry	Bözingenfeld	225
2585758.30489964	1219066.65906917	Port Thielle	Water	Port	226
2586523.80544287	1222173.31008976	Altersheim-Redenweg	Health	Bözingen	227
2587318.10545237	1221262.51008333	Südstrasse	Suburb	Mett	228
2584827.50162955	1220544.0030259	Viaductstrasse	Residential	Center	229
2583485.01084233	1219996.27017444	Vingelz	Water	Lake	230
2584343.00380114	1219491.20705779	Nidau-Lac	Water	Lake	231
2586114.41959549	1221490.07372696	Champagne-Blumen	Residential	Champagne	232
2585629.80489579	1220272.85907468	Madretsch-Zukunft	Residential	Madretsch	233
2588901.70491557	1223116.25907924	Bözingenfeld	Industry	Bözingenfeld	234
2586192.80543981	1222205.11009077	Altersheim-Reid	Health	Ried	235
2587030.50544646	1222540.76009019	Taubenloch	Taubenloch	Bözingen	236
2588914.00491459	1223573.88408117	Rolex	Industry	Bözingenfeld	237
2585060.75434641	1220902.38306997	Museum	Green	Center	238
2584367.50054306	1219403.5010082	Nidau-Wald	Forest	Nidau	239

Table 7.2: Summary of sensor locations, grouped by type, neighborhood, and sensor ID.

7.3 Metadata Sheet

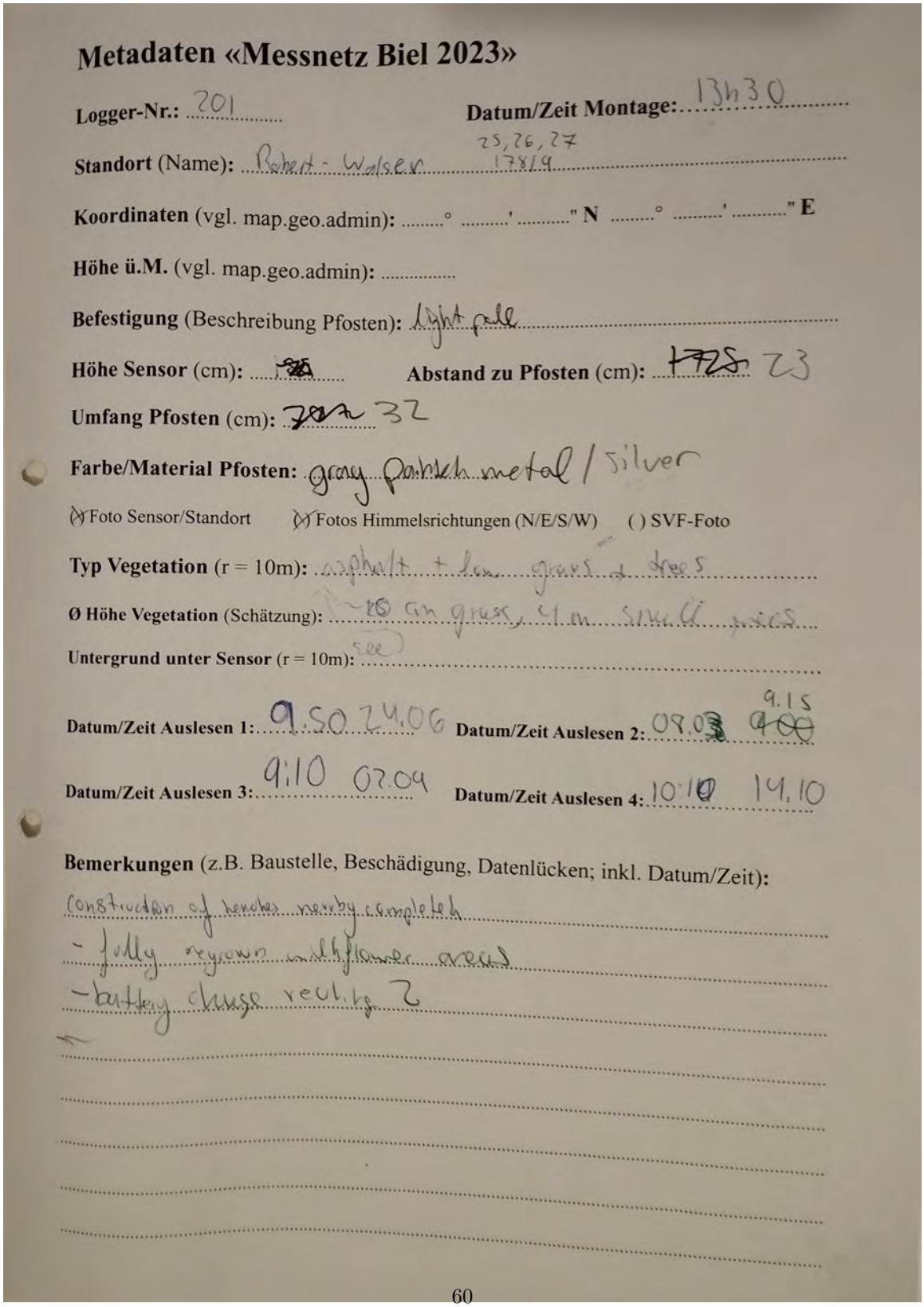

Metadaten «Messnetz Biel 2023»

Logger-Nr.: 201 **Datum/Zeit Montage:** 13h30

Standort (Name): Robert - Walser 25, 26, 27 17819

Koordinaten (vgl. map.geo.admin): .....° ....' ....." **N** .....° ....' ....." **E**

Höhe ü.M. (vgl. map.geo.admin): .....

Befestigung (Beschreibung Pfosten): light pole

Höhe Sensor (cm): ~~95~~ **Abstand zu Pfosten** (cm): ~~175~~ 23

Umfang Pfosten (cm): ~~20~~ 32

Farbe/Material Pfosten: grey painted metal / silver

(X) Foto Sensor/Standort (X) Fotos Himmelsrichtungen (N/E/S/W) ( ) SVF-Foto

Typ Vegetation (r = 10m): asphalt + low grass + trees

Ø Höhe Vegetation (Schätzung): ~20 cm grass, 4 m silver maple

Untergrund unter Sensor (r = 10m): see

Datum/Zeit Auslesen 1: 9.50 24.06 **Datum/Zeit Auslesen 2:** 09.03 9.15 9.00

Datum/Zeit Auslesen 3: 9:10 02.09 **Datum/Zeit Auslesen 4:** 10:10 14.10

Bemerkungen (z.B. Baustelle, Beschädigung, Datenlücken; inkl. Datum/Zeit):

construction of benches nearby completed
- fully regrown milkflower areas
- battery change recl. by Z

Figure 7.1: This is an example metadata sheet filled out during the sensor readings. Each sensor has its own metadata sheet.

7.4 Missing and Irregular Data

While only 4 of 39 sensors do not have a complete time series, it happens that these sensors correspond to lake and forest categories. In particular, there is no forest data available from May 15th - June 15th. Station 231 (Vingelz Lake) was not installed until June 06th, and is therefore missing data from May 15th until June 06th. A second issue is that a restuaranteer set up a food truck right underneath the station, contaminating the results with heat from food preparation during much of the summer season as well as highly modifying the terrain underneath the sensor. It changed from grass and gravel path to a large, square metal and plastic food truck.

Station 214 (Längholz Forest) was installed during the first round of data collection on June 14th 2023 due to issues with permissions for sensor placement. Data is therefore only available after this point. In addition, sometime after the second data collection, the radiation shield around the sensor was damaged and an additional sensor (logger 240) was set up in order to provide a reference. The damage likely came from falling branches during a storm, but the cause is not known. A back-up logger was installed next to logger 214 and the resulting data series for the last 3 weeks of the measurement campaign are presented in the results section. Station 239 (Nidau Forest) was installed on July 03rd 2023, as it was a delayed decision to expand the network to the forest on the lake shore. Therefore data is only available after this day. There are no other data issues.

Station 230 (Nidau Lake) did not begin collecting data until the first reading on June 19th 2023. A second interruption occurred from August 18th 2023 until August 31st 2023. The cause of the first period of missing data was due to operator error - during set-up the sensor was not started. The cause of the second interruption is unknown, especially as the sensor spontaneously restarted after about two weeks. The timing of the second interruption is quite unfortunate as this happened during the highest intensity part of the August heatwave.

7.5 Sensor 214 comparison

Forest station 214 exhibited a high number of summer days considering it is a forest station. Figure 5.7 shows the daily mean, minimum and maximum of the three forest sensors. Station 240 is a replacement affixed to the same tree as station 214 due to damage to 214's radiation shield. Station 239 is located in a small forest on the lake front. The results show that station 214 has generally higher maximums and lower minimums than station 239, with daily maximums sometimes reaching 5°C or higher than in the Nidau forest.

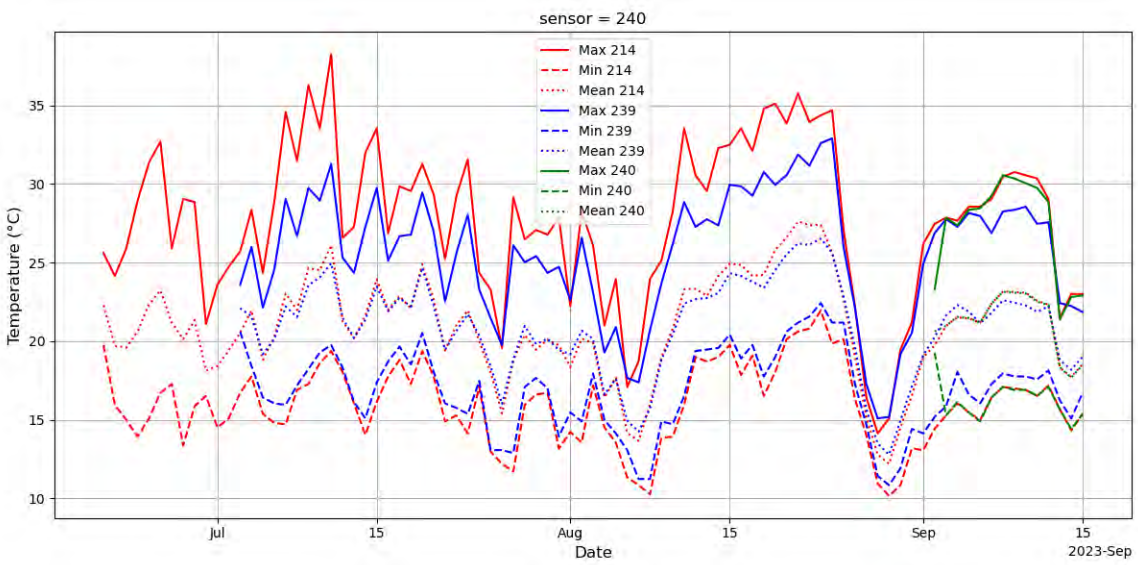

Figure 7.2: The comparison of the mean, min and maximum daily temperatures for the three sensors located in a forest reveals strong agreement between sensor 214 and sensor 240, despite the break in the radiation shield of sensor 214. It also reveals very high values for the station 214 and 240, compared to station 239.

7.6 bias

The sensor bias can also be seen using boxplots rather than ridge plots as presented in the main section of the paper.

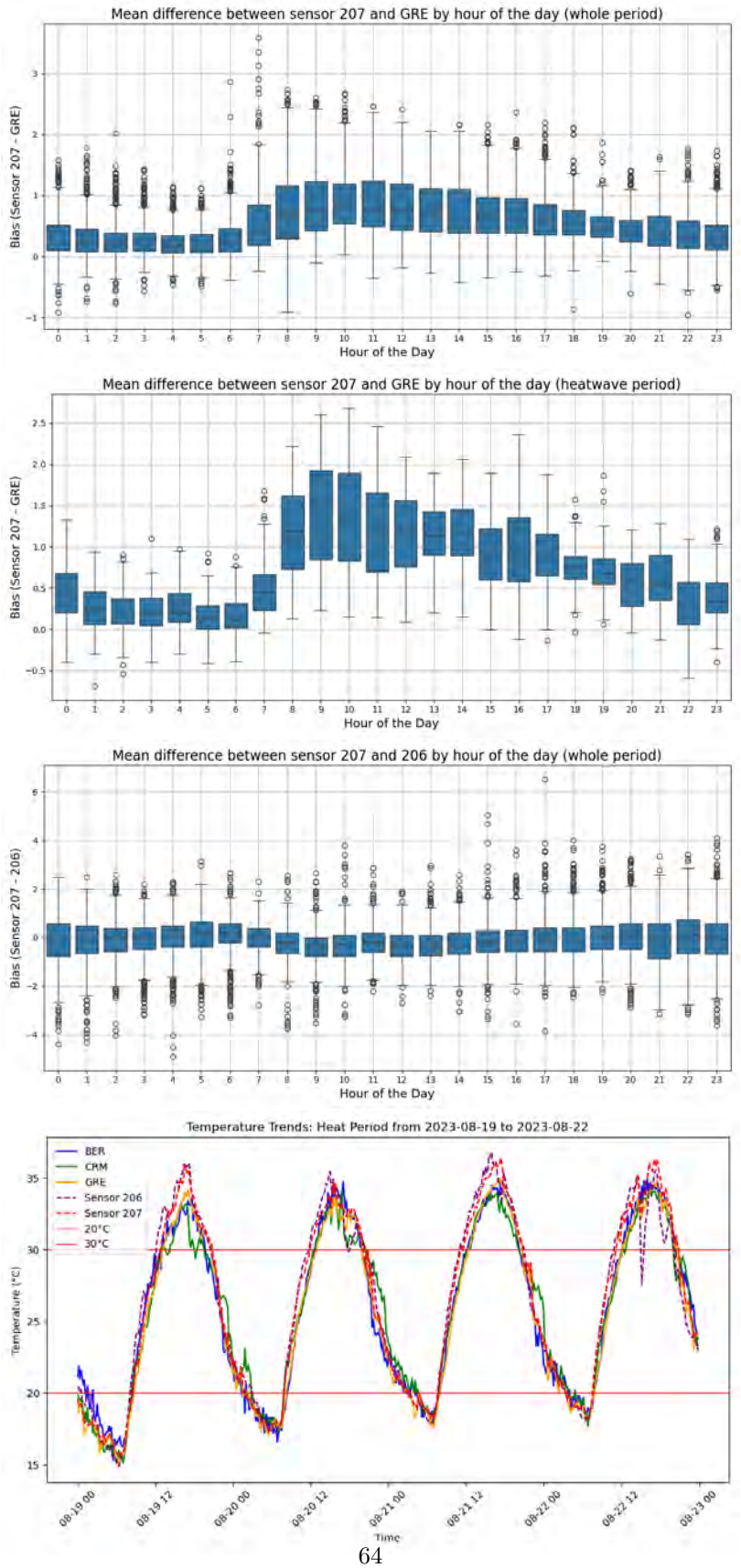

Figure 7.3: The top left figure shows the hourly boxplots of the difference between station 207 and the SwissMeteo AWS station at Grenchen airport averaged from May 15th - September 15th. The top right figure shows the same during the heatwave period of August 10th - 25th 2023. The bottom left figure shows the difference between the rural reference sensor 206 and the AWS reference sensor 207. The bottom right picture shows the actual data during a section of the heatwave period for

7.7 Fish Eye Photographs

The fish eye photographs can potentially be accessed through the GIUB. This example is for station 202 located on the Lake shore.

(a) Color SVF photo for station 202.

(b) Black and White SVF for station 202

Figure 7.4: The original SVF photo and the partially filtered SVF photo for station 202. This is the result of a semi-automated filter routine, but as can be seen each image needs additional manual touch-ups before they can be put to proper use.

7.8 2022 Charts

The main body of the thesis provides the data for 2023 and the 2022 data is presented here.

Figure 7.5: Reference data in 2022

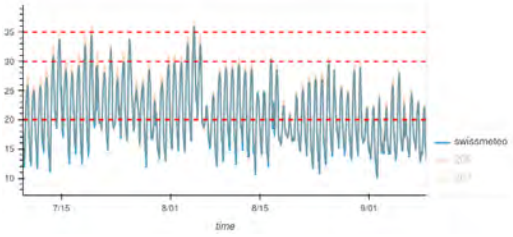

(a) Overall temperatures in 2022

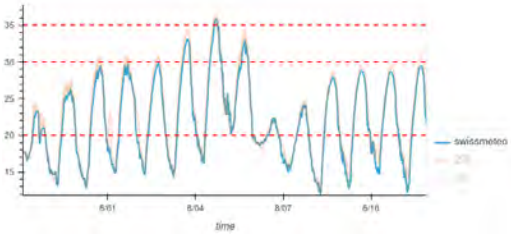

(b) Temperature evolution during short 2022 heatwave.

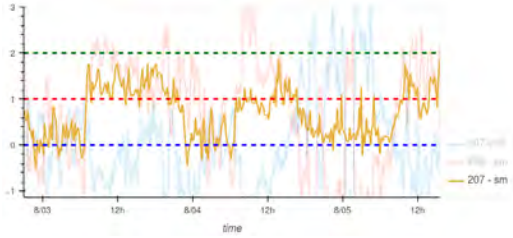

(c) Reference station differences during the early August 2022 heatwave.

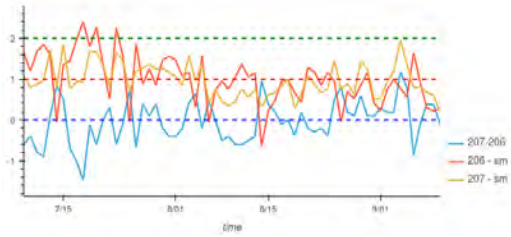

(d) Difference between daily minimum values at reference stations in 2022

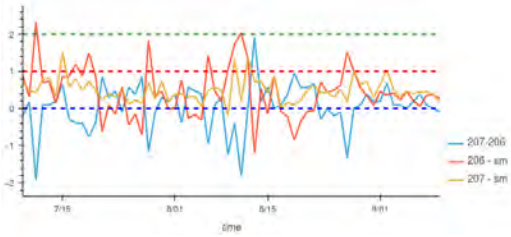

(e) Difference between daily minimum values at reference stations in 2022.

7.9 Tropical Nights

The full tropical nights heatmap is displayed for different thresholds.

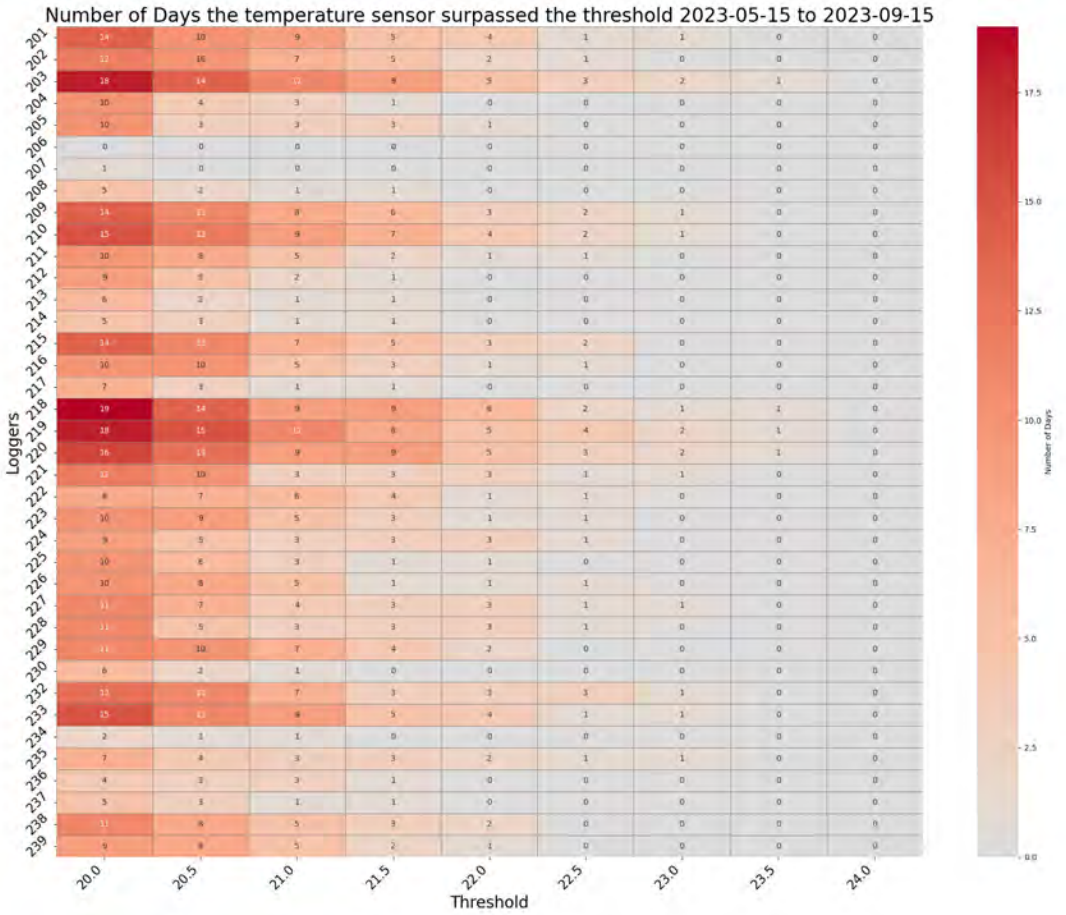

Figure 7.6: Number of days with a daily minimum that exceeded the threshold on the x axis. Note that sensors 214, 240, 239, and 230 are missing data for certain periods and therefore the number of possible summer days is reduced.

7.10 Warm and Summer Days

The full summer days heatmap is displayed for different thresholds.

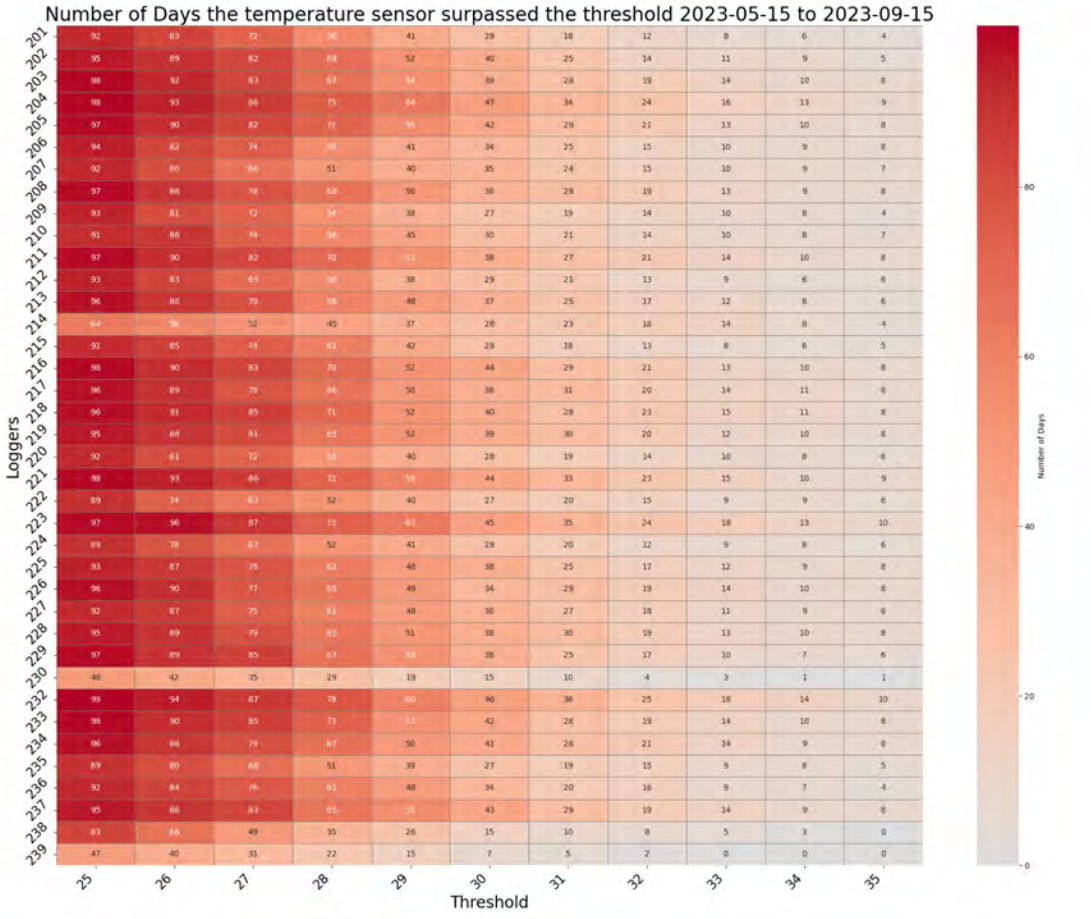

Figure 7.7: Number of days with a daily maximum that exceeded the threshold on the x axis. Note that sensors 214, 240, 239, and 230 are missing data for certain periods and therefore the number of possible summer days is reduced.

Declaration of consent

on the basis of Article 30 of the RSL Phil.-nat. 18

Name/First Name: Erismann, Gabrial

Registration Number: 21-112-990

Study program:

Bachelor ☐ Master ☒ Dissertation ☐

Title of the thesis: **Assessment of the Urban Heat Island in BielBienne**

Supervisor: Prof. Dr. Stefan Brönniman

I declare herewith that this thesis is my own work and that I have not used any sources other than those stated. I have indicated the adoption of quotations as well as thoughts taken from other authors as such in the thesis. I am aware that the Senate pursuant to Article 36 paragraph 1 litera r of the University Act of 5 September, 1996 is authorized to revoke the title awarded on the basis of this thesis.

For the purposes of evaluation and verification of compliance with the declaration of originality and the regulations governing plagiarism, I hereby grant the University of Bern the right to process my personal data and to perform the acts of use this requires, in particular, to reproduce the written thesis and to store it permanently in a database, and to use said database, or to make said database available, to enable comparison with future theses submitted by others.

Place/Date

Biel 20.01.2025

Signature

Gabrial Erismann